The E3 ubiquitin ligase HOS1 participates in the control of photoperiodic flowering in Arabidopsis negatively regulating CONSTANS abundance

Ana Lazaro[1], Federico Valverde[2], Manuel Piñeiro[1], Jose A. Jarillo[1,3]

[1] Centro de Biotecnología y Genómica de Plantas (CBGP), INIA-UPM. Instituto Nacional de Investigación y Tecnología Agraria y Alimentaria, Campus de Montegancedo, 28223 Madrid, Spain.

[2] Instituto de Bioquímica Vegetal y Fotosíntesis, Consejo Superior de Investigaciones Científicas y Universidad de Sevilla. Américo Vespucio 49, 41092 Sevilla, Spain.

[3] To whom correspondence should be addressed. e-mail: jarillo@inia.es

Telephone: 34-91-3364576; Fax 34-91-7157721

Running title: HOS1 regulates CO abundance

Key words: HOS1, E3 ubiquitin ligase, CONSTANS, flowering time, floral repression, Arabidopsis.

Estimated article length: 16,6 pages

SINOPSIS (400 characters long)

The regulation of *CONSTANS* (*CO*) gene expression is crucial to measure accurately the changes in daylength that influence flowering time in Arabidopsis. *CO* is under both transcriptional and post-translational control. Here we demonstrate that *ESD6/HOS1* is required to modulate precisely the timing of CO accumulation. This regulation is essential to maintain low levels of *FT* expression during the first part of the day and a correct photoperiodic response in Arabidopsis.

ABSTRACT

The *early in short days 6* (*esd6*) mutant was isolated in a screening devoted to isolate mutations that accelerate flowering time in Arabidopsis. Among other developmental alterations, *esd6* displays early flowering in both long and short day conditions. Fine mapping of the mutation showed that *esd6* was affected in the *HIGH EXPRESSION OF OSMOTICALLY RESPONSIVE GENES 1 (HOS1)* locus, which encodes a RING finger-containing protein that works as an E3 ubiquitin ligase. *esd6/hos1* mutation causes decreased expression of the *FLC* gene and shows a strong requirement of a functional CO protein for its early flowering phenotype under long days. Besides, CO and HOS1 physically interact *in vitro* and *in planta*, and HOS1 is regulating CO abundance, particularly during the daylight period. Accordingly, *hos1* mutation causes a shift in the regular long day pattern of expression of *FT* transcript, starting to rise four hours after dawn. In addition, *HOS1* interacts synergistically with *COP1*, another regulator of CO protein stability, in the control of flowering time. Taken together, these results indicate that HOS1 is involved in the control of CO abundance, ensuring that CO activation of *FT* occurs only when the light period reaches a certain length and preventing precocious flowering in Arabidopsis.

INTRODUCTION

The integration of complex signals from environmental and endogenous cues is necessary to enable plants to time the floral transition at the most advantageous moment (Michaels, 2009; de Montaigu et al., 2010; Imaizumi, 2010). Plants growing at northern latitudes adapt their developmental program to the varying daylengths and temperatures that occur along the year (Jackson, 2009). Arabidopsis is a facultative long-day (LD) plant in which flowering time is controlled by a network of six major pathways: information about daylength, low winter temperatures and growth temperature are mediated by the photoperiod, the vernalization and the ambient temperature pathway, respectively. In contrast, the aging, the autonomous and the gibberellin pathways act more independently of ambient conditions (Fornara et al., 2010). A potent repressor of flowering, *FLOWERING LOCUS C* (*FLC*), integrates signals coming from both the vernalization and the autonomous pathway (Amasino, 2010). Eventually, the whole network converges in the regulation of the floral integrators: *FLOWERING LOCUS T* (*FT*), *TWIN SISTER OF FT* (*TSF*) and *SUPPRESSOR OF OVEREXPRESSION OF CONSTANS 1* (*SOC1*) (Fornara et al., 2010).

The photoperiod pathway comprises several genes, including *GIGANTEA* (*GI*), *CONSTANS (CO)*, and *FT* (Kobayashi and Weigel, 2007; Turck et al., 2008). Mutations in any of these genes cause a delay in flowering mainly under LDs, whereas their overexpression accelerates flowering independently of daylength (Turck et al., 2008). CO is a B-box-type protein that acts in the vascular tissue of the leaves to activate *FT* and *TSF* transcription (An et al., 2004; Jackson, 2009; Tiwari et al., 2010). CO may induce *FT* expression by forming a DNA binding complex with NUCLEAR FACTOR Y (NF-Y)/HEME ACTIVATOR PROTEIN (HAP) proteins (Wenkel et al., 2006; Kumimoto et al., 2010) or ASYMMETRIC LEAVES 1 (AS1) (Song et al., 2011), and

by binding the *FT* promoter directly at CO-responsive elements (Tiwari et al., 2010), which are functional cis-elements required for *FT* expression (Adrian et al., 2010). FT protein, and possibly TSF, are part of the florigen that moves to the shoot apical meristem to induce flowering in response to LDs (Corbesier et al., 2007; Jaeger and Wigge, 2007; Jang et al., 2009).

Plants have developed a sophisticated molecular mechanism to measure daylength based on the coincidence of an internal rhythm, set by the circadian clock, with an external cue, such as light. The ability to distinguish LDs from short days (SDs) is largely the result of the complex regulation of *CO*, both at the transcriptional and post-translational level and may have arisen very early in plant evolution (Serrano et al., 2009; Valverde, 2011). Under LDs, *CO* mRNA shows two peaks of expression, the first following the expression of *GI* at the end of a LD, when plants are still exposed to light; and the second during the night. Under SDs, only the night peak of *CO* expression takes place (Suarez-Lopez et al., 2001). The precise timing of *CO* also requires the degradation of a family of repressors, the CYCLING DOF FACTORS (CDFs), by the F-Box proteins FLAVIN-BINDING, KELCH REPEAT, F-BOX 1 (FKF1), ZEITLUPE (ZTL) and LOV KELCH PROTEIN 2 (LKP2), in conjunction with GI (Imaizumi et al., 2005; Sawa et al., 2007; Fornara et al., 2009).

The increased expression of *CO* in the light under LDs but not SDs is crucial for the promotion of flowering, because exposure to light is required for stabilization of CO protein (Valverde et al., 2004; Jang et al., 2008). The high *CO* transcript levels detected during the dark phase of both LD and SDs do not correlate with CO protein accumulation because the RING finger protein CONSTITUTIVE PHOTOMORPHOGENIC 1 (COP1) promotes CO degradation in the dark (Jang et al., 2008; Liu et al., 2008b). Mutations in *COP1*, encoding a component of an ubiquitin

ligase complex, cause extreme early flowering under SDs. This early flowering phenotype is largely dependent on CO activity and correlates with an increase in *FT* transcription in the *cop1* mutant (Jang et al., 2008; Liu et al., 2008b). COP1 and CO interact both *in vivo* and *in vitro*, and it has been proposed that COP1 contributes to daylength perception by reducing the abundance of the CO protein during the night (Jang et al., 2008; Liu et al., 2008b; Chen et al., 2010). However, in the morning, CO degradation occurs independently of COP1 (Jang et al., 2008). Therefore, it has been suggested that an unidentified E3 ubiquitin ligase must collaborate in CO degradation during the early part of the day to ensure that CO induction of *FT* only takes place in LDs (Jang et al., 2008).

In addition to the length of the daily light/dark periods, plants also perceive light quality. Blue and far-red light promote flowering, while red light (RL) delays it (Valverde et al., 2004). Far-red light can increase CO protein levels independently of transcription (Kim et al., 2008). Blue light mediates photoperiodic control of the floral initiation at least by three different mechanisms: first, it promotes the interaction of FKF1 and GI necessary for the CDFs degradation (Sawa et al., 2007); second, the blue light receptor Cryptochrome 2 (Cry2) prevents GI and CO proteolysis by COP1 (Liu et al., 2008b; Yu et al., 2008) and a blue light-dependent interaction of CRY2 with SPA1 regulates COP1 activity (Zuo et al., 2011) ; and third, Cry2 modulates *FT* transcription directly (Liu et al., 2008a). On the other hand, the red light photoreceptor Phytochrome B (PhyB) has been implicated in the degradation of CO during the first part of the day (Valverde et al., 2004; Jang et al., 2008).

Screenings devoted to the isolation of early flowering mutants have revealed the existence of genes that repress the floral transition (Pouteau et al., 2004). Floral repressors are essential to safeguard against premature flowering, and knowledge of

how these repressors interact with the floral promotion pathways is just emerging (Pouteau et al., 2004; Roux et al., 2006). Here we demonstrate that the *esd6* early flowering mutant is affected in the *HOS1* gene. *HOS1* encodes a protein with E3 ubiquitin ligase activity, previously described as a regulator of cold acclimation responses (Lee et al., 2001; Dong et al., 2006a). The early flowering phenotype of *hos1* is completely suppressed by mutations in *CO* gene in Landsberg *erecta* (L*er*) background and notably delayed by *co* mutations in Columbia (Col) background. Moreover, we show that HOS1 physically interacts with CO *in vitro* and *in planta* and regulates CO protein abundance during the daylight period, indicating the participation of another RING finger-containing protein, in addition to COP1, in the photoperiodic control of flowering time in Arabidopsis. Thus, we propose that HOS1 is required to modulate precisely the timing of CO accumulation, and that this regulation is essential to maintain low levels of *FT* during the first part of the day and, subsequently, a correct photoperiodic response in Arabidopsis.

METHODS

1. Genetic stocks and growth conditions

Arabidopsis thaliana (L.) mutant seed stocks used were in L*er*, Col and C24 genetic backgrounds and were obtained from the Arabidopsis Biological Resource Centre (ABRC) of Ohio State University (Columbus, USA), the Nottingham Arabidopsis Centre (NASC) in the UK, and personal donations. C24 accession and mutant *hos1-1* seeds were kindly donated by Dr. J.K. Zhu (Lee et al., 2001). The monogenic mutants used in this work were described previously: *fca-1*, *ft-1*, *co-2* and *gi-3* (Koornneef, 1991); *fve-3* (Ausin et al., 2004); *flc-3* (Michaels and Amasino, 1999); *phyB-1* (Reed et al., 1993); *fha-1* (Guo et al., 1998); *vrn1-2 fca-1* (Levy et al., 2002); *vin3-4 FRI* Sf-2 (Sung and Amasino, 2004); *fld-1* (He et al., 2003); *siz1-2* (Miura et al., 2005); *fkf1-1* (Nelson et al., 2000); *cop1-4* (Deng et al., 1991); *co-10* (Laubinger et al., 2006); *soc1-1* (Samach et al., 2000); and the Col *FRI* Sf-2 line was described by Lee and Amasino (Lee and Amasino, 1995).

Plants were grown in plastic pots containing a mixture of substrate and vermiculite (3:1) or in MS (Murashige and Skoog) medium supplemented with 1% (w/v) sucrose and 0.8% (w/v) agar for *in vitro* culture. Controlled environmental conditions were provided in growth chambers at 22°C and 70% relative humidity. Plants were illuminated with cool-white fluorescent lights (approximately 120 µmol m^{-2} s^{-1}). LD conditions consisted of 16 h of light followed by 8 h of darkness; SD conditions consisted of 8 h of light followed by 16 h of darkness.

2. Phenotypic analysis

Total leaf number was scored as the number of leaves in the rosette (excluding cotyledons) plus the number of leaves in the inflorescence at the time of opening of the first flower (Koornneef, 1991). Cauline, adult and juvenile leaves were scored

independently. Rosette leaves lacking abaxial trichomes were considered as juvenile leaves (Telfer et al., 1997). Data are shown as mean ± s.e.m.

Root length was measured at different developmental stages in seedlings grown in MS medium supplemented with 1% (w/v) sucrose and 1% (w/v) plant agar in Petri dishes placed vertically.

Total chlorophyll content (Ct) was calculated as described by Moran (Moran, 1982).

3. Map-based cloning of *esd6* mutation and molecular characterization of the *hos1* alleles

A mapping population was generated from the crossing of the *esd6* mutant, in L*er* background, and a Col wild-type plant. The analysis of 550 early flowering plants with several polymorphic molecular markers (Supplemental Table 1) located the *esd6* mutation to the upper arm of chromosome 2, between markers C005 and T5I7. Mutations *hos1-1*, in C24 background, *hos1-2*, in L*er* background, and *hos1-4*, in Col background, generate premature stop codons in the seventh, fifth and first exon of the *HOS1* locus respectively. The T-DNA insertion mutant *hos1-3*, isolated in Col background, was obtained from NASC (SALK_069312).

4. Genetic analysis

Double mutants were constructed by crossing the monogenic *hos1* mutants with lines carrying the mutations *flc-3, fca-1, fve-3, fld-1, siz1-2, fha-1, gi-3, co-2, co-10, cop1-4, fkf1-1, ft-1, soc1-1, vrn1-2* or *vin3-4*. Double mutants were isolated from selfed F2 progeny using molecular markers. A dCAP marker was designed for the *hos1-2* mutation (PCR amplification using 5´-TTTTTACATGGCCGGTTCAGATC-3´ and 5´-GCAATGTAATGTGAAACTAGGCGA-3´ primers followed by *Bgl*II digestion). For the *hos1-3* mutation we used 5´-GGTTTCTGGACCGCATATTTC-3´, 5´-GGCTTCTGACCAGAGAGTGTT-3´ and the SALK LB1 primer. *hos1-3* was also

crossed with lines carrying the *FRI* Sf-2 allele (Lee and Amasino, 1995) and the *35S*::*CO* transgene (Simon et al., 1996).

5. Expression analysis

Total RNA was isolated using TRIzol (Invitrogen-Gibco) and reverse transcriptase-mediated PCR was performed according to described procedures (Martin-Trillo et al., 2006). For semiquantitative RT-PCR analysis the *HOS1* specific primers, 5´-TTGTCCTCTATTTGCGTTTGT-3´ and 5´-TCAAATTGGGGAAGAAGTTATG-3´, were designed to amplify the N-terminal part of the *HOS1* coding region. The *FLC*, *CO*, *FT* and *SOC1* probes used were described elsewhere (Pineiro et al., 2003; Lazaro et al., 2008). *UBIQUITIN 10* (*UBQ10*) was used as a loading control in these experiments. Quantitative real-time PCR (Q-PCR) analyses were performed using FastStart Universal SYBR Green Master (Roche) and protocols and primers already described for analyzing the expression of *CO*, *FT*, *SOC1* and *β-ACTIN* (*ACT*) genes (Chiang et al., 2009; Morris et al., 2010).

6. In vitro pull-down assays

The pMAL and the pMAL-HOS1 constructs were expressed in *Escherichia coli BL21* Rosetta strain and the proteins, Maltose Binding Protein (MBP) or MBP-HOS1, were purified on amylose resin (New England Biolabs). *In vitro* transcription/translation *CO* reactions were performed with the TNT Quick Coupled Transcription/Translation System (Promega) in the presence of ^{35}S-methionine (Amersham Biosciences). For pull-down assays, 1 mg of MBP or MBP-HOS1 bound to beads was incubated with 15 µl of the TNT reaction in 200 µl of binding buffer containing 50mM Hepes (pH 7.4), 1mM EDTA, 150 mM NaCl, 10% (v/v) glycerol, 0.1% (v/v) Tween-20, and 0.5 mM DTT (Dong et al., 2006a). The mixture was incubated at room temperature for 1 h and then washed five times with washing buffer (50 mM Tris pH 7.5, 150 mM NaCl, 0.2% (v/v)

Nonidet P-40). Samples were boiled in the presence of Laemmli buffer and analyzed by SDS-PAGE followed by autoradiography.

7. Bimolecular fluorescence complementation (BiFC) studies

HOS1 and CO complete ORFs were cloned in pYFN43 and pYFC43 vectors to produce HOS1 fused to the N terminal part of the Yellow Fluorescent Protein (YFN-HOS1), and CO fused to the C terminal part of the YFP (YFC-CO). These constructs were introduced into *Agrobacterium tumefaciens* strain C58C1. 5-week old *Nicotiana benthamiana* or 3-week old *A. thaliana* Nossen (No-0) plants were leaf-inoculated with YFC-CO and YFN-HOS1, the negative control pairs (YFC-CO coexpressed with YFN-AKIN β and YFC-AKIN 10 with YFN-HOS1) or a positive control (amino and carboxy parts of AKINβ and AKIN10 Sucrose non fermenting (Snf1)-related kinases (SnRK) (Ferrando et al., 2001), following protocols previously described (Voinnet et al., 2003). Fluorescent interactions were visualized under a Leica TCS SP2 confocal microscopy set at 550 nm. Images were analysed employing Leica LCSLite software.

8. Nuclear protein extraction and immunological experiments

Nuclei were isolated from frozen Arabidopsis seedlings grown in MS plates for two weeks. Plants were grinded with mortar and pestle in the presence of liquid nitrogen and 30 ml of nuclei isolation buffer containing 50 mM MES-KOH pH 8.0, 1 mM EDTA pH 8.0, 30% (v/v) glycerol, 5% (w/v) sucrose, 50 mM KCl, 10 mM MgCl2, 10 mM PMSF, 0.1% (v/v) Triton-100 and plant protease inhibitor cocktail (SIGMA). The slurry was filtered through 100 μm mesh and centrifuged sequentially at 6.000 rpm for 20 min; 5.000 rpm for 10 min and 4.000 rpm for 10 min in a Beckman Avanti J-26 XP centrifuge at 4°C employing JA-25.50 rotor, being the supernatant discarded in each step and the pellets resuspended in the same nuclei isolation buffer. The final pellet was resuspended in 1.5 ml of the same buffer omitting the detergent and centrifuged at 2.000

g in a microfuge at 4ºC. For immunoblot experiments, the nuclei-enriched preparation was disrupted in the presence of 6M guanidine chlorhydrate with circular stirring at 4°C, sonicated in a Brandson sonifier set at 10 W and centrifuged at 20.000 g 10 min in a microfuge at 4°C. The supernatant was precipitated with 90% (v/v) ethanol, recentrifuged at the same speed for 10 min and washed 3 times in 90% (v/v) ethanol. The final pellet was dried and resuspended in Laemmli loading buffer and loaded into 4-12% (w/v) acrylamide gels. Immunoblots were performed as described before, using CO antibodies (Valverde et al., 2004), and anti-H3 antibodies (AbCAM) as loading controls. Immuno-chemiluminescence signals were visualized and quantified using a ChemiDoc system (Bio-Rad).

For immunoprecipitation assays, nuclei-enriched preparations were suspended in high salt buffer (SIGMA Cell-Lytic kit) including 1/100 SIGMA plant protease inhibition cocktail for four h at 4°C and disrupted by sonication as before. Extracts were centrifuged at 20,000 g in a microfuge at 4°C and the supernatant dialyzed against MES (pH 8.0) 50 mM; Nonidet P-40 0.5 % (v/v); glycerol 10 % (v/v); EDTA (pH 8,0) 0.5 mM; PMSF 1 mM; 1/100 SIGMA plant protease inhibition cocktail; DTT 1 mM and B-mercapthoethanol 10 mM, 4 h, at 4°C. Protein extracts (100 µg) were incubated with 50 µl of anti GFP-Trap-A slurry (Chromotek) in the presence of 0.5 mM MG132 proteasome inhibitor at 4ºC overnight and proteins were processed following the instructions of the manufacturer. Eluted samples were run on a 10% (w/v) acrylamide/bis-acrylamide SDS-PAGE gel and Western blots performed employing anti-CO and anti-Ub antibodies as described before (Valverde et al., 2004).

9. Luciferase activity assays

A *35S*::*CO-LUC* construct was transformed in Col plants and homozygous lines were established. Several independent transgenic plants exhibiting early flowering

phenotype were selected and one representative line was crossed with *hos1-3* plants. For non-invasive *in vivo* luciferase (LUC) imaging, 10 day-old Col and *hos1-3* seedlings harbouring the *35S::CO-LUC* construct were grown in MS plates and sprayed with 100 μM luciferin (Biotium) 3h after dawn. The imaging system consisted of a PHOTON COUNTING I-CCD VIDEO CAMERA C2400-32 (Hammamatsu Photonics) mounted in a dark chamber. Image acquisition and processing were performed with the WASABI software provided by the camera manufacturer.

Quantification of luciferase activity was assayed on seedlings grown in the same conditions described above with a MicroBeta TriLux Luminometer (PerkinElmer). Seedlings were grinded in liquid nitrogen and resuspended in Steadylite Plus Reagent (PerkinElmer). The luciferase activity was measured as a mean of three independent experiments and expressed as luciferase counts per second (LCPS) in serial dilutions of fresh tissue in Steadylite Plus Reagent (mg/ml).

10. Subcellular localization of HOS1.

hos1-3 mutant plants were transformed with a *35S::HOS1-GFP* construct and the selected transgenic plants were grown in MS medium supplemented with 1% (w/v) sucrose and 1% (w/v) plant agar in Petri dishes placed vertically. 10 day-old transgenic plants grown under continuous light or dark conditions were analyzed by confocal microscopy (Zeiss LSM 710). DAPI staining of the nuclei was done at a final concentration of 10 μg/ml with 0.1% (v/v) Tween-20.

RESULTS

esd6 **mutant is early flowering and displays pleiotropic defects in both vegetative and reproductive development**

A recessive mutation that accelerated flowering time, named *early in short days 6* (*esd6*), was identified in a screening of a L*er* mutagenized population. Plants homozygous for *esd6* were selected as early flowering under LD conditions, although the *esd6* mutation also accelerated flowering under non inductive SD photoperiods (Figure 1A and B and Table 1). Earliness of *esd6* was mainly associated to the production of fewer leaves during the adult vegetative phase (Figure 1D) based on leaf trichome distribution (Telfer et al., 1997).

Besides their flowering phenotype, *esd6* mutant plants also displayed complex pleiotropic alterations of both vegetative and reproductive development. Mutant plants were smaller than wild-type (Figure 1A and B) and showed reduced leaf size compared to L*er* (Figure 1E). Moreover, *esd6* primary root was shorter and produced less secondary roots than the wild-type (Figure 1G and Supplemental Figure 1). In contrast, the stem length was not noticeably affected by the *esd6* mutation (Figure 1C). *esd6* flowers also displayed some developmental abnormalities including a reduced size in comparison to wild-type flowers (Figure 1F and Supplemental Figure 1). Besides, siliques were approximately 30% shorter in *esd6* mutant than in L*er* (Figure 1F and Supplemental Figure 1).

Because *esd6* mutant looked paler than L*er* (Figure 1H), we decided to measure the total chlorophyll content (Ct) present in both genotypes. We included *phyB-1* as a control in this experiment, since *phyB* mutants display a reduced chlorophyll accumulation (Reed et al., 1993). As expected, both *phyB-1* and *esd6* mutant showed

14

less Ct than L*er* (Figure 1H), indicating an additional role of *ESD6* gene in the control of chlorophyll biosynthesis.

The *ESD6* gene encodes HOS1, an E3 ubiquitin ligase

esd6 was identified in a L*er* transposon-mutagenized population generated from the genetic cross between two transgenic L*er* plants, one containing the *Ds (Dissociation)* element, and the other the transposase gene, capable of mobilizing the *Ds* element. The selection of *esd6* mutant was carried out in the F2 population where plants with different phenotypes were observed due to the mobilization of the transposon. We first noticed that the *esd6* early flowering phenotype did not cosegregate with the selection resistance gene. For this reason, we considered that the mutation was originated due to a second mobilization event of the *Ds* element that left a fingerprint in the genome. Consequently, to understand the molecular function of *ESD6,* we carried out a map-based cloning approach. *ESD6* was initially located in the upper arm of chromosome 2 and further linkage analyses allowed us to define a candidate region between C005 and T5I7 molecular markers, which encompassed eight open reading frames (ORFs) (Figure 2A). Among these loci, *HOS1* (*At2g39810*) had already been described as a regulator of cold acclimation responses also affecting flowering time (Lee et al., 2001). The sequencing of this transcription unit in *esd6* revealed a single nucleotide deletion in the position 2212 (fifth exon) which generated a premature stop codon (Figure 2B). To confirm that *esd6* was indeed affecting the same locus as the *hos1-1* mutation, we performed an allelism test. The F1 plants derived from the cross between *hos1-1*, in C24 background, and *esd6* mutant resulted to be early flowering, indicating that both mutations were allelic (Table 1). *esd6* mutant was referred to hereafter as *hos1-2*. In addition, we searched for T-DNA insertional alleles within the *HOS1* locus and

identified the line SALK_069312, which carried an insertion in the fifth exon of *HOS1* gene (Figure 2B). This T-DNA mutant allele was named *hos1-3* and, an additional allele, *hos1-4* was obtained later on in our laboratory during the screening of an EMS-mutagenized population of Col plants. *hos1-4* mutation created a single nucleotide deletion in the position 88 of the *HOS1* genomic annotation, which generated a premature stop codon in the first exon of the gene (Figure 2B). All *hos1* alleles analysed display an early flowering phenotype both in LD and SD photoperiods, but the fact that they flower earlier under inductive photoperiods, indicates that the mutation does not completely abolish the plant photoperiod response (Figure 2C and Table 1).

The *AtHOS1* gene is around 5.5 Kb long, bears 9 exons and encodes a protein of 915 amino acids that contains a non-canonical RING finger domain in the N-terminal region and a putative nuclear localization signal in the C-terminal part (Figure 2B and Supplemental Figure 2). *AtHOS1* is a unique gene in Arabidopsis and putative orthologues have only been found in plants. The cysteine residues present in the RING finger domain are totally conserved between all AtHOS1 orthologues (Supplemental Figure 2). RING finger domains are found in proteins with E3 ubiquitin ligase activity that participate in the ubiquitin/26S proteasome pathway (Deshaies and Joazeiro, 2009; Vierstra, 2009). Previously, it has been described that AtHOS1 can function as an E3 ubiquitin ligase in ubiquitination assays (Dong et al., 2006a).

hos1 mutations affect *FLC* expression and have an *FLC*-independent effect in the control of flowering time

The early flowering phenotype of *hos1* mutants suggested that HOS1 could be a negative regulator of the floral transition in Arabidopsis. To test this hypothesis, we analyzed the phenotype of double mutants carrying *hos1* and different mutations

affecting flowering time. It had been previously described that *FLC* expression levels were reduced in the *hos1-1* mutant compared to C24 accession (Lee et al., 2001). In order to check if the *hos1* early flowering phenotype was fully dependent on *FLC*, the effect of *hos1-3* mutation in an *flc* null genetic background (*flc-3*) (Michaels and Amasino, 1999) was tested. Both *hos1-3* and *hos1-3 flc-3* double mutant plants flowered with the same number of leaves, irrespectively of photoperiodic conditions, although the *hos1-3 flc-3* plants bolted consistently earlier than *hos1-3* under LD (Figure 3A and Table 1). This result may indicate that there is no additional effect of *flc* null mutation on the acceleration of flowering time caused by *hos1*. Besides, both *hos1-3* and *hos1-3 flc-3* plants flowered clearly earlier than *flc-3* plants under both LD and SD conditions (Figure 3A and Table 1), indicating that the effect of the *hos1* mutation on flowering time could not be exclusively dependent on *FLC* activity, and that there is an *FLC*-independent effect responsible for the early flowering phenotype of *hos1*. To find out whether *FLC* expression was altered in the *hos1* mutant alleles isolated in different backgrounds, semiquantitative RT-PCR analyses were performed in *hos1-1*, *hos1-2*, and *hos1-3* mutants and the corresponding wild-type genotypes. Consistently with previous results (Lee et al., 2001), in all *hos1* mutants assayed, *FLC* transcript was clearly down-regulated (Figure 3B), and therefore it cannot be ruled out that this change in *FLC* expression has an effect on the early flowering time of the *hos1* alleles.

Dominant alleles of the *FRIGIDA (FRI)* gene confer a vernalization requirement that delays flowering through the up-regulation of *FLC* (Johanson et al., 2000). In order to find out the genetic relationship between *HOS1* and *FRI*, the mutant *hos1-3* was crossed with a Col plant bearing an active *FRI* allele introgressed from the San Feliu-2 (Sf-2) accession (Lee and Amasino, 1995). Under LD conditions, the *hos1-3 FRI* Sf-2 line showed an additive phenotype, the *FRI* late-flowering phenotype being only

partially suppressed by *hos1-3* (Figure 3D upper panel and Table 1). This suggests that *HOS1* and *FRI* do not regulate *FLC* expression through the same pathway in LDs. In contrast, the *hos1-3 FRI* Sf-2 plant flowered with approximately the same number of leaves as the Col *FRI* Sf-2 plants under SD conditions, abolishing the effect of the *hos1* mutation (Figure 3D lower panel and Table 1).

Because *HOS1* locus is involved in cold signal transduction (Lee et al., 2001) and vernalization regulates *FLC* expression (Amasino, 2010), we hypothesized that *HOS1* could be controlling *FLC t*ranscript levels through the vernalization pathway. To analyze this, we generated combinations between *hos1* and two other mutants impaired in the vernalization response such as *vernalization 1 (vrn1)* and *vernalization-insensitive 3 (vin3)* (Levy et al., 2002; Sung and Amasino, 2004), both in late flowering backgrounds that allowed us to observe the acceleration of flowering due to the vernalization treatment. The *hos1* mutation did not impair the acceleration of flowering caused by vernalization when combined with the late flowering *fca-1* or *FRI* Sf-2 plants (Supplemental Table 2). Besides, no difference in flowering time was found for the *hos1-2 vrn1-2 fca-1* triple mutant grown after either 1 or 4 weeks of vernalization treatment (Supplemental Table 2). The same result was observed for *hos1-3 vin3-4* carrying an active *FRI* allele, as both 1 and 4 week-vernalized plants flowered with approximately the same number of leaves (Supplemental Table 2). Thus, we concluded that *HOS1* does not regulate *FLC* expression through the vernalization pathway.

Considering that the autonomous pathway also converges on the regulation of *FLC* expression, the flowering phenotype of double mutants combining *hos1* and mutations in representative autonomous pathway genes was analysed, in particular the *hos1-3 fve-3*, *hos1-2 fca-1* and *hos1-3 fld-1* double mutants. Under LD, these double mutant plants showed an additive phenotype because the late-flowering phenotype of autonomous

pathway mutants was only partially suppressed by *hos1* (Figure 3C upper panel and Table 1). In contrast, under SDs, flowering time of these double mutants was very similar to the one displayed by the autonomous pathway mutants, as they produced only a few leaves less than *fve-3*, *fca-1* and *fld-1* respectively (Figure 3C lower panel and Table 1).

Altogether, these results indicate that the *hos1* mutation cannot accelerate flowering in SD when combined with genetic backgrounds that have very high *FLC* expression levels, such as mutations of the autonomous pathway or active alleles of *FRI*. In contrast, under LD the repressive effect of *HOS1* on flowering time may be mediated by additional pathways that remain inactive in SD.

The E3 SUMO ligase SIZ1 promotes *FLC* expression by repressing the autonomous pathway gene *FLD* (Jin et al., 2008). Besides, SIZ1 stabilizes the ICE1 protein, which has been implicated in the regulation of freezing tolerance in Arabidopsis (Miura et al., 2007). Because it had been described that ICE1 was also targeted by HOS1 (Dong et al., 2006a), we checked the genetic relationship existing between *hos1* and *siz1* mutants. Flowering time of *siz1* plants relative to wild-type was slightly earlier under LDs, and substantially earlier under SDs (Jin et al., 2008) (Table 1). When we combined *siz1-2* with the *hos1-2* mutation, the double mutant flowering time resembled that of *hos1-2* in LDs but was earlier than any of the parental lines in SDs, suggesting a synergistic genetic interaction between both loci (Table 1).

The early flowering phenotype of *hos1-2* requires a functional *CO* gene

We also analyzed the phenotype of double mutants carrying *hos1* and mutations in genes representative of the photoperiod pathway, such as *CRY2/FHA*, *GI* and *CO*, that delay flowering mainly under LDs (Koornneef et al., 1998). While *hos1-2 fha-1* and

hos1-2 gi-3 double mutants showed an additive flowering phenotype between *hos1-2* and *fha-1* and *gi-3* late flowering mutants, the genetic interaction observed between *hos1-2* and *co-2* was completely different (Figure 4 and Table 1). Under LDs, the *hos1-2* mutation did not accelerate flowering time when it was combined with *co-2* (Figure 4C and Table 1); indeed, *hos1-2 co-2* plants flowered with the same number of leaves as *co-2* mutant, indicating a strong requirement of a functional *CO* gene for the early flowering phenotype of *hos1-2*. However, under SD conditions *hos1-2 co-2* flowered as early as *hos1-2* (Table 1), given that *co* mutations do not delay flowering under this photoperiodic condition. These genetic results suggest that *HOS1* is involved in the photoperiodic control of flowering time as a negative regulator of CO under LDs.

FKF1 is an F-Box protein (Imaizumi et al., 2005) that mediates the cyclic degradation of CDF proteins, which are repressors of *CO* expression (Imaizumi et al., 2005; Fornara et al., 2009). To study if there was any genetic interaction between *FKF1* and *HOS1,* the double mutant *hos1-3 fkf1-1*was analyzed and it showed an additive phenotype between the late flowering time of *fkf1-1* and the early flowering phenotype of *hos1-3* in LDs (Table 1). This result indicates that *HOS1* does not participate in the *FKF1* transcriptional regulatory pathway that controls *CO* expression.

hos1 mutants show an altered pattern of *FT* expression

FLC acts repressing the expression of the floral integrators *FT* and *SOC1*, while the photoperiod pathway activate *FT* and *SOC1* expression through *CO* (Yoo et al., 2005; Searle et al., 2006; Turck et al., 2008). Because *hos1* mutations showed downregulation of *FLC* expression (Figure 3B) and the *co-2* mutation was epistatic to *hos1-2* under LDs (Figure 4C), we decided to check the genetic relationship between *HOS1* and the floral integrators *FT* and *SOC1*. The *hos1-2 ft-1* double mutant showed a similar flowering

phenotype to *ft-1* under LD conditions, suggesting a strong requirement of *FT* by the *hos1* early flowering phenotype (Figure 5A and Table 1). In contrast, *hos1-2 soc1-1* double mutant was additive between both parental lines in both LD and SD conditions (Figure 5A and Table 1). This result is in accordance with the epistasis observed between *co-2* and *hos1-2*, considering that *FT* is the main target of CO under LDs (Yoo et al., 2005). In order to check whether the whole effect of *HOS1* on flowering time was through *FT* and *SOC1*, we generated the triple mutant *hos1-2 ft-1 soc1-1*. Flowering time analysis showed that the triple mutant was slightly earlier than *ft-1soc1-1* (Figure 5A and Table 1). This result indicates that the early flowering phenotype of *hos1* mutation requires functional *FT* and *SOC1* genes, although we cannot rule out that HOS1 could regulate other protein(s) involved in the control of flowering time.

In order to deepen into the genetic relationship observed between *HOS1* and the photoperiod pathway, we performed a time course expression analysis over a 24h period in L*er* and *hos1-2* seedlings both in LD and SD. First of all, we demonstrated that *HOS1* transcript did not show a diurnal oscillation in L*er* background (Figure 5B). Subsequently, we analyzed the temporal expression pattern of *CO*, *FT* and *SOC1* genes using semiquantitative RT-PCR and quantitative real-time PCR (Q-PCR) approaches (Fig 5C-E). As previously reported, *CO* transcript level in L*er* background was high at dawn and dusk, and during the night, remaining low for the rest of the light period of the day (Suarez-Lopez et al., 2001) (Fig 5C-E). In *hos1-2*, the same pattern of *CO* expression was observed, indicating that *hos1* mutation did not affect significantly the levels or the expression profile of the *CO* transcript (Figure 5C-E). However, the expression pattern of the floral integrator *FT* was clearly altered in the *hos1-2* mutant compared to the wild-type both in LD and SD conditions (Fig 5C-E). *FT* transcript usually shows a peak of expression at dusk in LDs (around ZT16), following the

evening increase observed in *CO* mRNA. In the *hos1-2* mutant, a peak of *FT* expression in the subjective morning, mainly at ZT4, but also at ZT8 was observed, when the *CO* transcript levels are barely detectable in the mutant (Figure 5C and D). To check whether this alteration was due to a specific developmental stage of the plant or if it relied on the genetic background, *FT* transcript levels were analysed at ZT4 and ZT8 in Col and *hos1-3* plants harvested 8, 10, 12 and 15 days after germination (DAG). In every single stage tested, *FT* expression was higher in *hos1-3* in relation to Col in the first part of the day (Supplemental Figure 3). In SD, an increased *FT* expression in the *hos1-2* mutant, starting to rise at ZT8 and peaking at ZT12 was observed, which may explain the early flowering phenotype displayed by the mutant under non-inductive photoperiods (Figure 5C and E). A small but consistent increase in *SOC1* expression was also detected in *hos1-2* plants grown in LD photoperiods in comparison to the wild-type (Figure 5C and D). Thus, we conclude that *CO* transcript levels are not modified substantially by the *hos1* mutation and that *HOS1* is required to repress the expression of *FT* in the first part of the day in LD. Considering that HOS1 has an E3 ubiquitin ligase activity, we speculated that it may be involved in the degradation of protein(s) that regulate *FT* expression. Both the genetic analysis and the expression assays suggested that this protein could be CO.

HOS1 interacts *in vitro* and *in vivo* with CO and regulates its abundance

Given the proposed epistatic interaction between *co-2* and *hos1-2* mutants and considering that *CO* transcript levels were not affected in the *hos1-2* mutant, we decided to analyze whether there was a physical interaction between CO and HOS1. For this purpose, *in vitro* pull-down experiments using MBP-HOS1 and *in vitro*-translated CO protein were performed. As shown in Figure 6A, MBP-HOS1, but not MBP alone, was

able to interact with CO protein. Whether the interaction between CO and HOS1 also occurred *in vivo* was tested using the bimolecular fluorescence complementation (BiFC) technique. For that, the N terminus of YFP was cloned upstream of HOS1 (YFN-HOS1) and the C terminus of YFP was fused to CO (YFC-CO). By *Agrobacterium tumefaciens* coinfiltration, these constructs were transiently expressed in abaxial epidermal cells of tobacco and Arabidopsis leaves (Voinnet et al., 2003). Reconstitution of YFP fluorescence was examined by confocal microscopy two days after transient coexpression of the protein pairs. Yellow fluorescence in the nucleus was detected for coexpression of YFC-CO and YFN-HOS1, while no yellow fluorescence was observed when YFC-CO was coexpressed with YFN-AKIN β, or when YFC-AKIN10 was coexpressed with YFN-HOS1, as negative controls (Figure 6B). As a positive control, the interaction between amino and carboxy parts of AKINβ and AKIN10 SnRKs proteins (Ferrando et al., 2001), was tested (Figure 6B). CO-HOS1 interaction could be observed in conspicuous nuclear speckles, which have been often associated with foci of proteasome degradation, as previously described for the interaction between CO and COP1 (Jang et al., 2008). These results demonstrate that CO and HOS1 colocalize and physically interact in the nuclei of plant cells.

The interaction between HOS1 and CO proteins was further explored by *in vivo* co-immunoprecipitation analysis. For this experiment, we generated *35S::HOS1-GFP* transgenic plants in Col background and we also introduced this construct in *35S::CO* plants. Nuclear proteins isolated from two-week-old *35S::HOS1-GFP 35S::CO* and *35S::HOS1-GFP* plants, grown in LD and harvested at ZT4 in the presence of MG132 proteasome inhibitor, were immunoprecipitated after incubation with an anti-GFP antibody (Figure 6C). The eluted purified proteins were blotted and detected with anti-CO antibody. As shown in Figure 6C, CO antibody recognized a clear signal in nuclear

extracts from *35S::HOS1-GFP 35S::CO* (Elution HC, marked by an arrow) plants but not in control extracts from the *35S::HOS1-GFP* (Elution H) plants. Given their apparent molecular mass and the comigration with the input CO protein (marked with an arrow), which included 1/50 protein amount of the immunoprecipitated fraction (input HC), the recognized bands must correspond to CO protein. In this blot, a higher molecular mass CO form (asterisk, upper panel) could also be detected. Because HOS1 has been described as a RING-finger E3 ligase (Dong et al., 2006a), the same blot was probed with anti–Ubiquitin antibody, resulting in only the upper immunoprecipitated band being recognized (asterisk, lower panel). This result demonstrates that a fraction of the immunoprecipitated CO protein was ubiquitinated *in vivo*, further supporting the association between both proteins and pointing to a role of HOS1 in the proteasome-dependent degradation of CO.

It has been reported that HOS1 has auto-ubiquitination ligase activity *in vitro* and that it can also mediate the ubiquitination and degradation of ICE1 transcription factor (Dong et al., 2006a). To further analyze whether HOS1 may also regulate CO degradation *in vivo*, a construct constitutively expressing *CO* fused to *LUC* was transformed into wild-type Arabidopsis plants. One representative line, *35S::CO–LUC* 6-2, displaying an early flowering phenotype, was introduced into *hos1*-3 by genetic crossing. The *35S::CO–LUC* 6-2/*hos1-3* plants flowered earlier than either the *hos1-3* mutant or the *35S::CO–LUC* 6-2 plants, indicating that CO–LUC construct was fully functional (Supplemental Table 3). Using luciferase fluorescence *in vivo* imaging, we found that under LDs the CO protein levels were significantly lower in the wild-type than in the *hos1* mutant background three hours after dawn (ZT3) (Figure 6D), suggesting that the degradation of CO that occurs in the wild-type is impaired in the *hos1* mutant. Quantification of luciferase activity corroborated that CO protein

accumulated to higher levels in the *hos1* mutant than in the wild-type plants (Figure 6E). This accumulation of CO protein observed at ZT3 correlates with the early peak of *FT* expression present in the *hos1* mutant (Figure 5C and D and Supplemental Figure 3). To further assess the role of HOS1 in CO regulation, we performed western blot assays to detect CO protein in nuclear extracts from wild-type and *hos1-3* plants grown under LD photoperiods. In these immunoblots, CO protein was present at lower abundance in the wild-type than in the *hos1-3* mutant plants, particularly during the daylight period (Figure 6F). From these data, we conclude that HOS1 is involved in the photoperiodic regulation of flowering through the modulation of CO protein levels *in vivo*.

HOS1 is a nuclear-localized protein that acts in the phloem to regulate photoperiodic flowering

HOS1 protein is ubiquitously expressed in all plant tissues (Lee et al., 2001). Computer analysis of the HOS1 amino acid sequence predicted a nuclear localization signal in the C-terminus of the protein (Supplemental Figure 2). Previous reports localized HOS1 into the cytoplasm of transgenic Arabidopsis seedlings overexpressing a *HOS1-GFP* construct, grown under dark conditions at normal growth temperature. However, in response to low temperature treatments, HOS1-GFP accumulated in the nucleus (Lee et al., 2001). To determine whether the subcellular localization of HOS1 was altered by light/dark conditions, we overexpressed a *HOS1-GFP* construct in the *hos1-3* mutant. The homozygous line *35S::HOS1-GFP/hos1-3* 4-1-4 showed a delay in flowering time when compared with *hos1*-3, indicating that the fusion protein was functional in the repression of flowering (Figure 7 E). Subsequently, we grew *35S::HOS1-GFP/hos1-3* 4-1-4 transgenic plants at 22ºC under both continuous light and dark, and analyzed GFP fluorescence in root cells by confocal microscopy. As

shown in Figure 7A-C, HOS1-GFP was clearly targeted to the nucleus; whereas the fluorescence signal could be detected throughout the whole organelle, a significant fraction was localized to the nuclear envelope, independently of the light growing conditions. These results are in agreement with recent observations implicating HOS1 as an interactor of RNA export factor 1 (RAE1) nucleoporin (Tamura et al., 2010). Moreover, the nuclear localization of HOS1-GFP is also consistent with the results of the BiFC assay described above (Figure 6B) and with the detection of CO and other HOS1 targets in the nucleus (Valverde et al., 2004; Dong et al., 2006a).

Given the described interaction between CO and HOS1 (Figure 6) and because CO acts in the phloem companion cells to activate *FT* transcription (An et al., 2004), we tested whether HOS1 may also regulate flowering when specifically expressed in phloem tissue. Expression of *HOS1* under the control of the phloem companion cell-specific *SUC2* promoter (Imlau et al., 1999) in *hos1* mutant plants delayed their flowering time and caused partial complementation of the early-flowering phenotype of *hos1* mutant (Figure 7D-E). By contrast, expression of *HOS1* under the shoot apical meristem specific promoter of the *KNOTTED-LIKE FROM ARABIDOPSIS THALIANA 1 (KNAT1)* gene (Lincoln et al., 1994) in *hos1* mutant plants did not alter their flowering time (Figure 7D-E), demonstrating that *HOS1* expression is required in the phloem companion cells, where *CO* is expressed, to repress flowering.

HOS1 interacts synergistically with COP1 in the control of flowering time

COP1 E3 ubiquitin ligase is involved in the degradation of CO protein during the night (Jang et al., 2008; Liu et al., 2008b). However, CO degradation in the morning occurs independently of COP1 (Jang et al., 2008), and for this reason, we speculate that HOS1 may be involved in this process. In our conditions, *cop1-4* mutants flowered

dramatically earlier than wild-type and *hos1* plants under SDs. However, under LDs *cop1-4* mutants flowered earlier than Col, but later than *hos1* plants (Figure 8A and Table 1). To test the effect of abolishing the activity of both HOS1 and COP1 in the control of flowering time, *hos1* and *cop1* mutations were combined. Interestingly, the *hos1-3 cop1-4* double mutant flowered earlier than both parents in LD and SD, displaying the same number of leaves in both photoperiodic conditions (Figure 8A and Table 1). This result indicates that the combination of both mutations renders a plant with a complete loss of photoperiod sensitivity, and that *HOS1* and *COP1* genes are functionally related in the control of flowering time.

To further investigate the genetic interaction between *HOS1*, *COP1* and *CO* genes in controlling flowering time of Arabidopsis, a *hos1 cop1 co* triple mutant was generated and its flowering time was compared with that of *hos1 co* and *cop1 co* double mutants (Figure 8B and Table 1). Under LDs, the *hos1-3 co-10* and the *cop1-4 co-10* plants flowered with 12 and 10 leaves less than *co-10* respectively, indicating that part of the early flowering phenotype of the *hos1-3* and *cop1-4* mutants in Col background occurs independently of *CO*. This result appears to be in contrast with the epistatic genetic relationship observed between *hos1-2* and *co-2* alleles in L*er* background (Figure 4C and Table 1), and can be explained because *hos1* mutation is downregulating *FLC* expression (Figure 3B) and *FLC* is expressed at higher levels in Col than in L*er* (Michaels and Amasino, 1999). Besides, the *hos1 cop1 co* triple mutant flowered with 15 leaves more than the *hos1 cop1* double mutant under LD conditions, demonstrating that *co* mutation notably delays the *hos1 cop1* early flowering phenotype in Col background. Interestingly, the *hos1 cop1 co* triple mutant formed 6 and 9 leaves less than *hos1 co* and *cop1 co* double mutants respectively (Figure 8B and Table 1),

27

confirming the existence of a synergistic genetic interaction between *hos1* and *cop1*, even in the absence of *CO*.

Because *HOS1* seems to exert an effect as a negative regulator of *CO*, we tested whether the extremely early flowering of *35S::CO* plants (Simon et al., 1996) could be further accelerated by the *hos1-3* mutation. To test this hypothesis, the *35S::CO* transgene was introduced into wild-type Col and into *hos1-3* mutant plants. Although the number of leaves at flowering for both transgenic plants was very similar, we observed that the *hos1-3 35S::CO* plants bolted consistently earlier than the Col *35S::CO* (Figure 8C and Table 1), supporting a role for *HOS1* in repressing the promotion of flowering mediated by *CO*.

DISCUSSION

In many plants, changes in daylength regulate the transition from vegetative growth to flowering, and plants altered in the daylength-sensing mechanism cannot time flowering properly in natural environments (Wilczek et al., 2009). In this work, both genetic and molecular approaches demonstrate that *HOS1* is involved in the photoperiodic control of flowering time. The *esd6/hos1* mutant was identified through a screening designed to isolate early flowering mutants in Arabidopsis. The characterization of these mutants allows unveiling the mechanisms of action of genes involved in the repression of the floral transition and suggests that a large number of genes participate in this process (Pouteau et al., 2004). In addition to precocious flowering, the *hos1* mutant showed pleiotropic alterations of leaf, flower and root development, similarly to those displayed by other early flowering mutants (Martin-Trillo et al., 2006; del Olmo et al., 2010).

In Arabidopsis, the flowering response due to changes in photoperiod relies on the interaction of light with the circadian clock-regulated rhythmic expression of *CO* (Suarez-Lopez et al., 2001). Besides this transcriptional regulation, a light-dependent regulation of CO protein stability has also been described (Valverde et al., 2004; Kim et al., 2008). We have demonstrated that HOS1 is a nuclear-localized protein that acts in the phloem to repress flowering time (Figure 7) and that it is involved in regulating CO protein abundance *in vivo* (Figure 6), ensuring that CO activation of *FT* only occurs at the appropriate times of the day under inductive photoperiods in Arabidopsis. HOS1 has been reported to work as an E3 ubiquitin ligase that mediates the degradation of ICE1 transcription factor (Dong et al., 2006a), and we have demonstrated that CO interacts *in vitro* and *in planta* with HOS1, and that CO coimmunoprecipitates with HOS1 *in vivo* (Figure 6). In addition, *hos1* mutation altered *FT* expression pattern in LD, showing a

29

peak of expression in the subjective morning (Figure 5C and D). These observations suggest that HOS1 could mediate CO degradation during the daylight period through a mechanism involving ubiquitination, and that the timing of HOS1 activity is crucial to establish a photoperiodic flowering response (Figure 9). Both the genetic analysis between *CO* and *HOS1* genes (Figure 4) and the expression analyses performed involving *CO* transcript and CO protein (Figure 5-6), support this hypothesis.

Other E3 ubiquitin ligases have been proposed to be involved in the control of flowering time (Cao et al., 2008; Vega-Sanchez et al., 2008; Park et al., 2010). In particular, DAY NEUTRAL FLOWERING (DNF) and COP1 have been demonstrated to regulate the precise pattern of *CO* expression at the transcriptional and the posttranscriptional level respectively (Jang et al., 2008; Liu et al., 2008b; Morris et al., 2010). DNF is an important regulator of the rhythm of *CO* expression, but it is not acting through the GI/FKF1/CDFs regulatory mechanism (Morris et al., 2010). Increased CO transcript in the *dnf* mutant around ZT 4-6 results in an earlier induction of *FT* under SD (Morris et al., 2010). On the other hand, CO protein is degraded in the dark by the SUPPRESSOR OF PHYA-105 1 (SPA1)-COP1 complex (Laubinger et al., 2006; Jang et al., 2008; Liu et al., 2008b). Besides, it has been recently demonstrated that the Arabidopsis CULLIN4 E3 RING ligase bound to Damaged DNA Binding protein 1 (DDB1) interacts with SPA1-COP1 complex to regulate flowering time (Chen et al., 2010). We have demonstrated that *HOS1* also interacts genetically with *COP1* in the photoperiodic control of flowering time (Figure 8A). Interestingly, *hos1 cop1* double mutants are completely insensitive to photoperiod, and *co* mutations notably delay the early flowering phenotype of the *hos1 cop1* double mutant (Figure 8B). This can be interpreted as HOS1 and COP1 being functionally related proteins in the control of flowering time, regulating CO abundance during the day and in the night,

respectively (Figure 9). This is consistent with the observation that the absence of both E3 ubiquitin ligases renders plants unable to distinguish between LDs and SDs. It has been proposed that a phyB-dependent mechanism occurring early in the day may promote CO degradation as well, but the E3 ubiquitin ligase(s) involved in this process remains to be identified (Valverde et al., 2004; Jang et al., 2008). Our data are consistent with HOS1 playing a crucial role in preventing increased CO protein levels and *FT* expression during early hours of the day. Further analyses will be required to establish the possible participation of HOS1 in the proposed phyB-dependent mechanism of CO proteolysis.

The ability to respond to photoperiod enables plants to anticipate variations in environmental conditions that can be predicted to occur periodically each year. In northern latitudes, shortening daylength in autumn is associated to decreasing cold temperatures while warm temperatures are typical of longer days. In addition to repress the floral transition, HOS1 was previously described as a negative regulator of cold signal transduction (Lee et al., 2001). This suggests that HOS1 might function as an integrative link for both responses, allowing plants to discriminate the duration of the day by regulating CO abundance, and to respond to cold temperatures, by regulating *CBF* (*C-repeat (CRT)-binding factors*) expression through ICE1 degradation (Dong et al., 2006a). Several evidences point to the existence of overlapping pathways for controlling cold stress and flowering time responses in Arabidopsis (Yoo et al., 2007; Seo et al., 2009). The characterization of several mutants altered in cold acclimation responses has uncovered a role of the corresponding genes in flowering time control. *hos9* and *sensitive to freezing 6* (*sfr6)* mutants show a late flowering phenotype, while *long vegetative phase 1* (*lov1*) mutant is early flowering (Zhu et al., 2004; Yoo et al., 2007; Knight et al., 2008). These three genes regulate the expression of cold-inducible

genes independently of CBFs, and both *LOV1* and *SFR6* control flowering time through the photoperiod pathway. Other mutants, such as *low expression of osmotically responsive genes 4* (*los4*) and *atnup160*, display an early flowering phenotype and altered *CBF* expression levels (Gong et al., 2005; Dong et al., 2006b). On the other hand, *co* and *gi* photoperiod pathway mutants show altered tolerance to freezing temperatures (Cao et al., 2005; Yoo et al., 2007), and *fve* mutant flowers late and shows increased expression of *FLC* and *CBF* genes (Kim et al., 2004). It has been proposed very recently that in warm late spring SOC1 downregulates *CBFs* expression and promotes flowering, while in cold early spring or fall, induction of *FLC* expression by the CBFs delays flowering and confers cold resistance to the plant (Seo et al., 2009). Besides regulating CO stability, *HOS1* controls *FLC* expression (Figure 3B) (Lee et al., 2001), which is also repressed by prolonged exposure to cold temperatures (Amasino, 2010). The positive effect of *HOS1* on *FLC* expression appears to be independent of the vernalization pathway (Bond et al., 2011) (Supplemental Table 2) and is still uncharacterised. Taken together, these results suggest that HOS1, among other genes, may participate in the photoperiod and temperature signal crosstalk, integrating information coming from both pathways and facilitating a proper response to changing environmental conditions. To our knowledge this is the first E3 ubiquitin ligase proposed to integrate both environmental signals, specifically targeting for degradation key factors involved in the regulation of each response. Further studies will be necessary for an in-depth understanding of how these pathways modulate each other´s activity to optimize plant adaptation.

BIBLIOGRAPHY

Adrian, J., Farrona, S., Reimer, J.J., Albani, M.C., Coupland, G., and Turck, F. (2010). *cis*-Regulatory elements and chromatin state coordinately control temporal and spatial expression of *FLOWERING LOCUS T* in Arabidopsis. Plant Cell **22,** 1425-1440.

Amasino, R. (2010). Seasonal and developmental timing of flowering. Plant J **61,** 1001-1013.

An, H., Roussot, C., Suarez-Lopez, P., Corbesier, L., Vincent, C., Pineiro, M., Hepworth, S., Mouradov, A., Justin, S., Turnbull, C., and Coupland, G. (2004). CONSTANS acts in the phloem to regulate a systemic signal that induces photoperiodic flowering of Arabidopsis. Development **131,** 3615-3626.

Ausin, I., Alonso-Blanco, C., Jarillo, J.A., Ruiz-Garcia, L., and Martinez-Zapater, J.M. (2004). Regulation of flowering time by FVE, a retinoblastoma-associated protein. Nat Genet **36,** 162-166.

Bond, D.M., Dennis, E.S., and Finnegan, E.J. (2011). The low temperature response pathways for cold acclimation and vernalization are independent. Plant Cell Environ **34,** 1737-1748.

Cao, S., Ye, M., and Jiang, S. (2005). Involvement of *GIGANTEA* gene in the regulation of the cold stress response in Arabidopsis. Plant Cell Rep **24,** 683-690.

Cao, Y., Dai, Y., Cui, S., and Ma, L. (2008). Histone H2B monoubiquitination in the chromatin of *FLOWERING LOCUS C* regulates flowering time in Arabidopsis. Plant Cell **20,** 2586-2602.

Corbesier, L., Vincent, C., Jang, S., Fornara, F., Fan, Q., Searle, I., Giakountis, A., Farrona, S., Gissot, L., Turnbull, C., and Coupland, G. (2007). FT protein movement contributes to long-distance signaling in floral induction of Arabidopsis. Science **316,** 1030-1033.

Chen, H., Huang, X., Gusmaroli, G., Terzaghi, W., Lau, O.S., Yanagawa, Y., Zhang, Y., Li, J., Lee, J.H., Zhu, D., and Deng, X.W. (2010). Arabidopsis CULLIN4-Damaged DNA Binding Protein 1 Interacts with CONSTITUTIVELY PHOTOMORPHOGENIC1-SUPPRESSOR OF PHYA Complexes to Regulate Photomorphogenesis and Flowering Time. Plant Cell **22,** 108-123.

Chiang, G.C., Barua, D., Kramer, E.M., Amasino, R.M., and Donohue, K. (2009). Major flowering time gene, *FLOWERING LOCUS C*, regulates seed germination in *Arabidopsis thaliana*. Proc Natl Acad Sci U S A **106,** 11661-11666.

de Montaigu, A., Toth, R., and Coupland, G. (2010). Plant development goes like clockwork. Trends Genet **26,** 296-306.

del Olmo, I., Lopez-Gonzalez, L., Martin-Trillo, M.M., Martinez-Zapater, J.M., Pineiro, M., and Jarillo, J.A. (2010). *EARLY IN SHORT DAYS 7* (*ESD7*) encodes the catalytic subunit of DNA polymerase epsilon and is required for flowering repression through a mechanism involving epigenetic gene silencing. Plant J **61,** 623-636.

Deng, X.W., Caspar, T., and Quail, P.H. (1991). *cop1*: a regulatory locus involved in light-controlled development and gene expression in Arabidopsis. Genes Dev **5,** 1172-1182.

Deshaies, R.J., and Joazeiro, C.A. (2009). RING domain E3 ubiquitin ligases. Annu Rev Biochem **78,** 399-434.

Dong, C.H., Agarwal, M., Zhang, Y., Xie, Q., and Zhu, J.K. (2006a). The negative regulator of plant cold responses, HOS1, is a RING E3 ligase that mediates the ubiquitination and degradation of ICE1. Proc Natl Acad Sci U S A **103,** 8281-8286.

Dong, C.H., Hu, X., Tang, W., Zheng, X., Kim, Y.S., Lee, B.H., and Zhu, J.K. (2006b). A putative Arabidopsis nucleoporin, AtNUP160, is critical for RNA export and required for plant tolerance to cold stress. Mol Cell Biol **26,** 9533-9543.

Ferrando, A., Koncz-Kalman, Z., Farras, R., Tiburcio, A., Schell, J., and Koncz, C. (2001). Detection of *in vivo* protein interactions between Snf1-related kinase subunits with intron-tagged epitope-labelling in plants cells. Nucleic Acids Res **29,** 3685-3693.

Fornara, F., de Montaigu, A., and Coupland, G. (2010). SnapShot: Control of flowering in Arabidopsis. Cell **141,** 550 e551-552.

Fornara, F., Panigrahi, K.C., Gissot, L., Sauerbrunn, N., Ruhl, M., Jarillo, J.A., and Coupland, G. (2009). Arabidopsis DOF transcription factors act redundantly to reduce *CONSTANS* expression and are essential for a photoperiodic flowering response. Dev Cell **17,** 75-86.

Gong, Z., Dong, C.H., Lee, H., Zhu, J., Xiong, L., Gong, D., Stevenson, B., and Zhu, J.K. (2005). A DEAD box RNA helicase is essential for mRNA export and important for development and stress responses in Arabidopsis. Plant Cell **17,** 256-267.

Guo, H., Yang, H., Mockler, T.C., and Lin, C. (1998). Regulation of flowering time by Arabidopsis photoreceptors. Science **279,** 1360-1363.

He, Y., Michaels, S.D., and Amasino, R.M. (2003). Regulation of flowering time by histone acetylation in Arabidopsis. Science **302,** 1751-1754.

Imaizumi, T. (2010). Arabidopsis circadian clock and photoperiodism: time to think about location. Curr Opin Plant Biol **13,** 83-89.

Imaizumi, T., Schultz, T.F., Harmon, F.G., Ho, L.A., and Kay, S.A. (2005). FKF1 F-box protein mediates cyclic degradation of a repressor of *CONSTANS* in Arabidopsis. Science **309,** 293-297.

Imlau, A., Truernit, E., and Sauer, N. (1999). Cell-to-cell and long-distance trafficking of the green fluorescent protein in the phloem and symplastic unloading of the protein into sink tissues. Plant Cell **11,** 309-322.

Jackson, S.D. (2009). Plant responses to photoperiod. New Phytol **181,** 517-531.

Jaeger, K.E., and Wigge, P.A. (2007). FT protein acts as a long-range signal in Arabidopsis. Curr Biol **17,** 1050-1054.

Jang, S., Torti, S., and Coupland, G. (2009). Genetic and spatial interactions between *FT*, *TSF* and *SVP* during the early stages of floral induction in Arabidopsis. Plant J **60,** 614-625.

Jang, S., Marchal, V., Panigrahi, K.C., Wenkel, S., Soppe, W., Deng, X.W., Valverde, F., and Coupland, G. (2008). Arabidopsis COP1 shapes the temporal pattern of CO accumulation conferring a photoperiodic flowering response. EMBO J **27,** 1277-1288.

Jin, J.B., Jin, Y.H., Lee, J., Miura, K., Yoo, C.Y., Kim, W.Y., Van Oosten, M., Hyun, Y., Somers, D.E., Lee, I., Yun, D.J., Bressan, R.A., and Hasegawa, P.M. (2008). The SUMO E3 ligase, *AtSIZ1*, regulates flowering by controlling a salicylic acid-mediated floral promotion pathway and through affects on *FLC* chromatin structure. Plant J **53,** 530-540.

Johanson, U., West, J., Lister, C., Michaels, S., Amasino, R., and Dean, C. (2000). Molecular analysis of *FRIGIDA*, a major determinant of natural variation in Arabidopsis flowering time. Science **290,** 344-347.

Kim, H.J., Hyun, Y., Park, J.Y., Park, M.J., Park, M.K., Kim, M.D., Lee, M.H., Moon, J., Lee, I., and Kim, J. (2004). A genetic link between cold responses and flowering time through *FVE* in *Arabidopsis thaliana*. Nat Genet **36,** 167-171.

Kim, S.Y., Yu, X., and Michaels, S.D. (2008). Regulation of *CONSTANS* and *FLOWERING LOCUS T* expression in response to changing light quality. Plant Physiol **148,** 269-279.

Knight, H., Thomson, A.J., and McWatters, H.G. (2008). SENSITIVE TO FREEZING 6 integrates cellular and environmental inputs to the plant circadian clock. Plant Physiol **148,** 293-303.

Kobayashi, Y., and Weigel, D. (2007). Move on up, it's time for change mobile signals controlling photoperiod-dependent flowering. Genes Dev **21,** 2371-2384.

Koornneef, M. (1991). Isolation of higher plant developmental mutants. Symp Soc Exp Biol **45,** 1-19.

Koornneef, M., Alonso-Blanco, C., Peeters, A.J., and Soppe, W. (1998). Genetic Control of Flowering Time in Arabidopsis. Annu Rev Plant Physiol Plant Mol Biol **49,** 345-370.

Kumimoto, R.W., Zhang, Y., Siefers, N., and Holt, B.F., 3rd. (2010). NF-YC3, NF-YC4 and NF-YC9 are required for CONSTANS-mediated, photoperiod-dependent flowering in *Arabidopsis thaliana*. Plant J **63,** 379–391.

Laubinger, S., Marchal, V., Le Gourrierec, J., Wenkel, S., Adrian, J., Jang, S., Kulajta, C., Braun, H., Coupland, G., and Hoecker, U. (2006). Arabidopsis SPA proteins regulate photoperiodic flowering and interact with the floral inducer CONSTANS to regulate its stability. Development **133,** 3213-3222.

Lazaro, A., Gomez-Zambrano, A., Lopez-Gonzalez, L., Pineiro, M., and Jarillo, J.A. (2008). Mutations in the Arabidopsis *SWC6* gene, encoding a component of the SWR1 chromatin remodelling complex, accelerate flowering time and alter leaf and flower development. J Exp Bot **59,** 653-666.

Lee, H., Xiong, L., Gong, Z., Ishitani, M., Stevenson, B., and Zhu, J.K. (2001). The Arabidopsis *HOS1* gene negatively regulates cold signal transduction and encodes a RING finger protein that displays cold-regulated nucleo-cytoplasmic partitioning. Genes Dev **15,** 912-924.

Lee, I., and Amasino, R.M. (1995). Effect of Vernalization, Photoperiod, and Light Quality on the Flowering Phenotype of Arabidopsis Plants Containing the *FRIGIDA* Gene. Plant Physiol **108,** 157-162.

Levy, Y.Y., Mesnage, S., Mylne, J.S., Gendall, A.R., and Dean, C. (2002). Multiple roles of Arabidopsis *VRN1* in vernalization and flowering time control. Science **297,** 243-246.

Lincoln, C., Long, J., Yamaguchi, J., Serikawa, K., and Hake, S. (1994). A *knotted1*-like homeobox gene in Arabidopsis is expressed in the vegetative meristem and dramatically alters leaf morphology when overexpressed in transgenic plants. Plant Cell **6,** 1859-1876.

Liu, H., Yu, X., Li, K., Klejnot, J., Yang, H., Lisiero, D., and Lin, C. (2008a). Photoexcited CRY2 interacts with CIB1 to regulate transcription and floral initiation in Arabidopsis. Science **322,** 1535-1539.

Liu, L.J., Zhang, Y.C., Li, Q.H., Sang, Y., Mao, J., Lian, H.L., Wang, L., and Yang, H.Q. (2008b). COP1-Mediated Ubiquitination of CONSTANS Is

Implicated in Cryptochrome Regulation of Flowering in Arabidopsis. Plant Cell **20,** 292-306.

Martin-Trillo, M., Lazaro, A., Poethig, R.S., Gomez-Mena, C., Pineiro, M.A., Martinez-Zapater, J.M., Jarillo, J.A., (Print), -., Article, J., and Research Support, N.-U.S.G.t. (2006). *EARLY IN SHORT DAYS 1* (*ESD1*) encodes ACTIN-RELATED PROTEIN 6 (AtARP6), a putative component of chromatin remodelling complexes that positively regulates *FLC* accumulation in Arabidopsis. Development **133,** 1241-1252.

Michaels, S.D. (2009). Flowering time regulation produces much fruit. Curr Opin Plant Biol **12,** 75-80.

Michaels, S.D., and Amasino, R.M. (1999). *FLOWERING LOCUS C* encodes a novel MADS domain protein that acts as a repressor of flowering. Plant Cell **11,** 949-956.

Miura, K., Jin, J.B., Lee, J., Yoo, C.Y., Stirm, V., Miura, T., Ashworth, E.N., Bressan, R.A., Yun, D.J., and Hasegawa, P.M. (2007). SIZ1-Mediated Sumoylation of ICE1 Controls *CBF3/DREB1A* Expression and Freezing Tolerance in Arabidopsis. Plant Cell **19,** 1403-1414.

Miura, K., Rus, A., Sharkhuu, A., Yokoi, S., Karthikeyan, A.S., Raghothama, K.G., Baek, D., Koo, Y.D., Jin, J.B., Bressan, R.A., Yun, D.J., and Hasegawa, P.M. (2005). The Arabidopsis SUMO E3 ligase SIZ1 controls phosphate deficiency responses. Proc Natl Acad Sci U S A **102,** 7760-7765.

Moran, R. (1982). Formulae for determination of chlorophyllous pigments extracted with N,N-dimethylformamide. Plant Physiol **69,** 1376-1381.

Morris, K., Thornber, S., Codrai, L., Richardson, C., Craig, A., Sadanandom, A., Thomas, B., and Jackson, S. (2010). *DAY NEUTRAL FLOWERING* represses *CONSTANS* to prevent Arabidopsis flowering early in short days. Plant Cell **22,** 1118-1128.

Nelson, D.C., Lasswell, J., Rogg, L.E., Cohen, M.A., and Bartel, B. (2000). *FKF1*, a clock-controlled gene that regulates the transition to flowering in Arabidopsis. Cell **101,** 331-340.

Park, B.S., Eo, H.J., Jang, I.C., Kang, H.G., Song, J.T., and Seo, H.S. (2010). Ubiquitination of LHY by SINAT5 regulates flowering time and is inhibited by DET1. Biochem Biophys Res Commun **398,** 242-246.

Pineiro, M., Gomez-Mena, C., Schaffer, R., Martinez-Zapater, J.M., and Coupland, G. (2003). EARLY BOLTING IN SHORT DAYS is related to chromatin remodeling factors and regulates flowering in Arabidopsis by repressing *FT*. Plant Cell **15,** 1552-1562.

Pouteau, S., Ferret, V., Gaudin, V., Lefebvre, D., Sabar, M., Zhao, G., and Prunus, F. (2004). Extensive phenotypic variation in early flowering mutants of Arabidopsis. Plant Physiol **135,** 201-211.

Reed, J.W., Nagpal, P., Poole, D.S., Furuya, M., and Chory, J. (1993). Mutations in the gene for the red/far-red light receptor phytochrome B alter cell elongation and physiological responses throughout Arabidopsis development. Plant Cell **5,** 147-157.

Roux, F., Touzet, P., Cuguen, J., and Le Corre, V. (2006). How to be early flowering: an evolutionary perspective. Trends Plant Sci **11,** 375-381.

Samach, A., Onouchi, H., Gold, S.E., Ditta, G.S., Schwarz-Sommer, Z., Yanofsky, M.F., and Coupland, G. (2000). Distinct roles of CONSTANS target genes in reproductive development of Arabidopsis. Science **288,** 1613-1616.

Sawa, M., Nusinow, D.A., Kay, S.A., and Imaizumi, T. (2007). FKF1 and GIGANTEA Complex Formation is Required for Day-Length Measurement in Arabidopsis. Science **318,** 261-265.

Searle, I., He, Y., Turck, F., Vincent, C., Fornara, F., Krober, S., Amasino, R.A., and Coupland, G. (2006). The transcription factor FLC confers a flowering response to vernalization by repressing meristem competence and systemic signaling in Arabidopsis. Genes Dev **20,** 898-912.

Seo, E., Lee, H., Jeon, J., Park, H., Kim, J., Noh, Y.S., and Lee, I. (2009). Crosstalk between Cold Response and Flowering in Arabidopsis Is Mediated through the Flowering-Time Gene *SOC1* and Its Upstream Negative Regulator *FLC*. Plant Cell **21,** 3185-3197.

Serrano, G., Herrera-Palau, R., Romero, J.M., Serrano, A., Coupland, G., and Valverde, F. (2009). Chlamydomonas *CONSTANS* and the Evolution of Plant Photoperiodic Signaling. Curr Biol.

Simon, R., Igeno, M.I., and Coupland, G. (1996). Activation of floral meristem identity genes in Arabidopsis. Nature **384,** 59-62.

Song, Y.H., Lee, I., Lee, S.Y., Imaizumi, T., and Hong, J.C. (2011). CONSTANS and ASYMMETRIC LEAVES 1 complex is involved in the induction of *FLOWERING LOCUS T* in photoperiodic flowering in Arabidopsis. Plant J **69,** 332-342.

Suarez-Lopez, P., Wheatley, K., Robson, F., Onouchi, H., Valverde, F., and Coupland, G. (2001). *CONSTANS* mediates between the circadian clock and the control of flowering in Arabidopsis. Nature **410,** 1116-1120.

Sung, S., and Amasino, R.M. (2004). Vernalization in *Arabidopsis thaliana* is mediated by the PHD finger protein VIN3. Nature **427,** 159-164.

Tamura, K., Fukao, Y., Iwamoto, M., Haraguchi, T., and Hara-Nishimura, I. (2010). Identification and characterization of nuclear pore complex components in *Arabidopsis thaliana*. Plant Cell **22,** 4084-4097.

Telfer, A., Bollman, K.M., and Poethig, R.S. (1997). Phase change and the regulation of trichome distribution in *Arabidopsis thaliana*. Development **124,** 645-654.

Tiwari, S.B., Shen, Y., Chang, H.C., Hou, Y., Harris, A., Ma, S.F., McPartland, M., Hymus, G.J., Adam, L., Marion, C., Belachew, A., Repetti, P.P., Reuber, T.L., and Ratcliffe, O.J. (2010). The flowering time regulator CONSTANS is recruited to the *FLOWERING LOCUS T* promoter via a unique *cis*-element. New Phytol **187,** 57-66.

Turck, F., Fornara, F., and Coupland, G. (2008). Regulation and identity of florigen: FLOWERING LOCUS T moves center stage. Annu Rev Plant Biol **59,** 573-594.

Valverde, F. (2011). CONSTANS and the evolutionary origin of photoperiodic timing of flowering. J Exp Bot **62,** 2453-2463.

Valverde, F., Mouradov, A., Soppe, W., Ravenscroft, D., Samach, A., and Coupland, G. (2004). Photoreceptor regulation of CONSTANS protein in photoperiodic flowering. Science **303,** 1003-1006.

Vega-Sanchez, M.E., Zeng, L., Chen, S., Leung, H., and Wang, G.L. (2008). SPIN1, a K homology domain protein negatively regulated and ubiquitinated by the E3 ubiquitin ligase SPL11, is involved in flowering time control in rice. Plant Cell **20,** 1456-1469.

Vierstra, R.D. (2009). The ubiquitin-26S proteasome system at the nexus of plant biology. Nat Rev Mol Cell Biol **10,** 385-397.

Voinnet, O., Rivas, S., Mestre, P., and Baulcombe, D. (2003). An enhanced transient expression system in plants based on suppression of gene silencing by the p19 protein of tomato bushy stunt virus. Plant J **33,** 949-956.

Wenkel, S., Turck, F., Singer, K., Gissot, L., Le Gourrierec, J., Samach, A., and Coupland, G. (2006). CONSTANS and the CCAAT box binding complex share a functionally important domain and interact to regulate flowering of Arabidopsis. Plant Cell **18,** 2971-2984.

Wilczek, A.M., Roe, J.L., Knapp, M.C., Cooper, M.D., Lopez-Gallego, C., Martin, L.J., Muir, C.D., Sim, S., Walker, A., Anderson, J., Egan, J.F., Moyers, B.T., Petipas, R., Giakountis, A., Charbit, E., Coupland, G., Welch, S.M., and Schmitt, J. (2009). Effects of genetic perturbation on seasonal life history plasticity. Science **323,** 930-934.

Yoo, S.K., Chung, K.S., Kim, J., Lee, J.H., Hong, S.M., Yoo, S.J., Yoo, S.Y., Lee, J.S., and Ahn, J.H. (2005). *CONSTANS* activates *SUPPRESSOR OF OVEREXPRESSION OF CONSTANS 1* through *FLOWERING LOCUS T* to promote flowering in Arabidopsis. Plant Physiol **139,** 770-778.

Yoo, S.Y., Kim, Y., Kim, S.Y., Lee, J.S., and Ahn, J.H. (2007). Control of flowering time and cold response by a NAC-domain protein in Arabidopsis. PLoS ONE **2,** e642.

Yu, J.W., Rubio, V., Lee, N.Y., Bai, S., Lee, S.Y., Kim, S.S., Liu, L., Zhang, Y., Irigoyen, M.L., Sullivan, J.A., Zhang, Y., Lee, I., Xie, Q., Paek, N.C., and Deng, X.W. (2008). COP1 and ELF3 control circadian function and photoperiodic flowering by regulating GI stability. Mol Cell **32,** 617-630.

Zhu, J., Shi, H., Lee, B.H., Damsz, B., Cheng, S., Stirm, V., Zhu, J.K., Hasegawa, P.M., and Bressan, R.A. (2004). An Arabidopsis homeodomain transcription factor gene, *HOS9*, mediates cold tolerance through a CBF-independent pathway. Proc Natl Acad Sci U S A **101,** 9873-9878.

Zuo, Z., Liu, H., Liu, B., Liu, X., and Lin, C. (2011). Blue Light-Dependent Interaction of CRY2 with SPA1 Regulates COP1 activity and Floral Initiation in Arabidopsis. Curr Biol **21,** 841-847.

ACKNOWLEDGEMENTS

FIGURE LEGENDS

Figure 1. Phenotypic characterization of the *esd6* mutant.

(A,B) Flowering time phenotype of L*er* and *esd6* plants grown in LD conditions for 23 days (A) or in SD conditions for 54 days (B). (C) Phenotype of L*er* and *esd6* plants grown in LD conditions for 35 days (D) Histograms comparing the number of juvenile, adult and cauline leaves in L*er* and *esd6* plants grown under both LD and SD photoperiods. (E) Rosette and cauline leaves of Ler and *esd6* plants grown in LDs. (F) Detached L*er* and *esd6* flowers and siliques from plants grown under LD conditions. (G) Root elongation in 11 day-old L*er* and *esd6* seedlings. (H) Total chlorophyll content (Ct) in L*er* and *esd6* and *phyB-1* mutant seedlings.

Figure 2. Identification of *ESD6*.

(A) Map-based cloning of *ESD6*. The genetic interval and the bacterial artificial chromosome (BAC) clones in the genomic region surrounding *ESD6* are shown. The number of recombinant events between molecular markers is given in parentheses. The position of *HOS1* ORF in T5I7 BAC clone is indicated. (B) Scheme of the *ESD6/HOS1* gene structure showing the polymorphisms associated to the different *hos1* mutant alleles isolated. Exons are represented by squared boxes, while introns are drawn by a line. (C) Pictures illustrating the flowering time of *hos1* mutants and their respective wild-type genotypes in LD and SD conditions. Plants were grown for 23 days under LD conditions (upper panel). SD pictures (lower panel) were taken after 64 days for C24 and *hos1-1*, 58 days for L*er* and *hos1-2* and 60 days for Col and *hos1-3*.

Figure 3. *hos1* mutations downregulate *FLC* expression and have an *FLC*-independent effect in the control of flowering time.

(A) Flowering time phenotype of *hos1-3 flc-3* double mutant in LD (upper panel) and SD (lower panel) conditions. (B) Analysis of the expression of *FLC* in 14 day-old *hos1* mutant seedlings and their corresponding wild-type genotypes. *FLC* expression was monitored by semiquantitative RT-PCR analysis over 22 cycles for C24 and *hos1-1* and over 28 cycles for L*er*, *hos1-2*, Col and *hos1-3*. For the *UBQ10* control 22 cycles were used. (C) Flowering time phenotype of *hos1-3 fve-3* double mutant plants grown in LD (upper panel) and SD (lower panel) conditions. (D) Flowering time phenotype of *hos1-3* plants bearing an active allele of *FRI* in LDs (upper panel) and SDs (lower panel).

40

Figure 4. Genetic analyses between *hos1* and mutations in photoperiod pathway genes.

Flowering time phenotype of *hos1-2 fha-1* (A), *hos1-2 gi-3* (B) and *hos1-2 co-2* (C) double mutants grown in LD conditions.

Figure 5. The early flowering phenotype of *hos1* depends on FT and SOC1 functional proteins and *hos1* mutation alters the pattern of expression of *FT*.

(A) Flowering time phenotype of *hos1-2 soc1-1, hos1-2 ft-1* and *hos1-2 ft-1 soc1-1* triple mutant plants grown in LD conditions. (B) *HOS1* expression pattern over a 24h time course in L*er* seedlings grown for 8 days in LDs and for 16 days in SDs. Samples were harvested every 4h after dawn. *HOS1* expression was monitored by semiquantitative RT-PCR analysis over 20 cycles. (C, D, E) Expression analysis of different flowering time genes over a 24h time course in L*er* and *hos1-2* seedlings grown for 8 days in LDs and 16 days in SDs. Samples were harvested every 4h after dawn (C) Semiquantitative RT-PCR analysis comparing *CO* (22 cycles), *FT* (28 cycles) and *SOC1* (24 cycles) expression (D) Quantitative real- time PCR (Q-PCR) analysis of *CO*, *FT* and *SOC1* expression in LD conditions (E) Same as (D) but L*er* and *hos1-2* seedlings grown in SD conditions. Relative expression levels were normalized to *β-ACTIN* expression.

Figure 6. HOS1 interacts with CO and regulates its abundance.

(A) HOS1 and CO interact *in vitro*. A Coomassie stained SDS-PAGE showing MBP (42KDa) and MBP-HOS1 fusion protein (147KDa) expressed in *Escherichia coli BL21* Rosetta strain and purified on amylose resin is shown in the upper panel. The lower panel shows the result of a pull-down assay with MBP and MBP-HOS1 proteins incubated with ^{35}S-Met-labelled CO protein. Retained CO protein was visualized after autoradiography of the dried gel. (B) HOS1 interacts with CO *in planta*. BiFC assay co-expressing the C terminus of YFP fused to CO (CO-YFC) and the N terminus of YFP to HOS1 (YFN-HOS1) in tobacco and Arabidopsis leaves. Yellow fluorescence in the nucleus was indicative of interaction. Negative and positive controls were included in the assay. (C) *In vivo* coimmunoprecipitation between HOS1 and CO. GFP-HOS1 protein was immunoprecipitated from *35S::CO 35S::GFP-HOS1* (HC) and *35S::GFP-HOS1* (H) plants employing GFP antibody-agarose columns and detected with anti-CO

antibodies (Elution HC, upper panel). The arrow marks both the co-immunoprecipitated CO protein and input. Antibodies against ubiquitin recognized, in the same blot, a higher molecular mass band (asterisk) corresponding to an ubiquitinated CO form (Elution HC, lower panel). Controls included input (1/50) from HC and H samples as well as column flowthrough and washes. Protein markers are shown on the right. (D) Non invasive *in vivo* luciferase imaging of *35S::CO–LUC* 6-2 and *35S::CO–LUC* 6-2/*hos1-3* seedlings. Pictures show 7 day-old seedlings grown in LDs 3 h after the lights are on. At this time, more CO-LUC protein accumulates in *hos1* mutant (below right) than in the wild-type (below left). (E) Quantification of the luciferase activity in *35S::CO–LUC* 6-2 (blue bars) and *35S::CO–LUC* 6-2/*hos1-3* (grey bars) seedlings expressed as luciferase counts per second (LCPS) in serial dilutions of fresh tissue in Steadylite Plus Reagent (mg/ml). (F) Immunoblot showing CO protein levels during a 24 h time course in nuclear extracts from Col and *hos1-3* plants grown under LDs. Numbers above each lane represent hours after dawn that the sample was harvested. Histone H3 was used as a loading control. Relative quantification of each band compared to the control is expressed below the upper panel (α-CO).

Figure 7. HOS1 is a nuclear-localized protein that exerts an effect in the phloem to regulate photoperiodic flowering

Localization of HOS1-GFP in the root cells of 10-day old *35S::HOS1-GFP/hos1-3* plants analysed under confocal microscopy. (A) Plants grown under continuous light. (B) Plants grown in darkness. (C) A representative nuclear image of a light-grown seedling showing DAPI staining (upper panel), GFP fluorescence (middle panel) and the merge of both images (lower panel). Tissue specific expression of *HOS1* in phloem companion cells and in the shoot apical meristem of *hos1* transgenic plants. (D) Flowering time phenotype of Col, *hos1-3, SUC2::HOS1/hos1-3 and KNAT1::HOS1/hos1-3* plants in LD. (E) Quantification of flowering time of Col, *hos1-3, 35S::HOS1-GFP/hos1-3*, *SUC2::HOS1/hos1-3 and KNAT1::HOS1/hos1-3* plants grown in LD conditions. Total number of leaves was scored in approximately 10 plants and is represented as mean ± s.e.m.

Figure 8. Genetic interaction between *HOS1* and *COP1* in the control of flowering time.

(A) Flowering time phenotype of *hos1-3 cop1-4* double mutant in LD (upper panel) and SD (lower panel) conditions. (B) Flowering time phenotype of double and triple mutant combinations between *hos1-3 co-10 cop1-4* mutants grown in LD conditions. (C) Comparison of flowering time phenotype between LD-grown Col and *hos1-3* plants bearing a *35S::CO* transgene.

Figure 9. Model for HOS1 function in the photoperiodic control of flowering time.
The transcription of *CO* gene depends primarily on the circadian clock (thick black line). In the evening, the degradation of CDFs by the GI/FKF1 complex allows *CO* transcript levels to increase, and CO protein accumulates due to a photoreceptor-mediated repression of COP1. At this time CO can promote *FT* expression and induce flowering. During the night, COP1 activity causes rapid degradation of CO protein by the ubiquitination/26S proteasome system. In the daylight period HOS1 is required to degrade CO. Additional data will be necessary to establish the possible involvement of HOS1 in the mechanism of CO degradation mediated by PhyB that has been proposed to operate in the morning.

Table 1. Flowering time of *hos1* double mutants		
	LD	**SD**
C24	25,6 ± 3,7	56,3 ± 7,2
hos1-1 (C24)	11,9 ± 2,2	38,7 ± 7,0
Ler	8,4 ± 0,9	24,1 ± 3,3
hos1-2 (Ler)	6,7 ± 0,9	17,6 ± 1,9
Col	13 ± 1,1	71,8 ± 6,5
hos1-3 (Col)	7,2 ± 0,5	32,5 ± 6
hos1-1 x hos1-2 (F1)	8,1 ± 1	
flc-3 (Col)	9,1 ± 0,6	61,9 ± 12,7
hos1-3 flc-3	6,8 ± 0,4	33,7 ± 6,7
Col FRI Sf-2	61,7 ± 9,6	121,3 ± 21,6
hos1-3 FRI Sf-2	40,9 ± 6,8	129,9 ± 16,4
fca-1 (Ler)	33,3 ± 4,5	84,6 ± 11,2
hos1-2 fca-1	15,4 ± 1,8	79,9 ± 10,8
fve-3 (Col)	42,8 ± 6,1	108,4 ± 11,8
hos1-3 fve-3	13,6 ± 1,1	94,6 ± 9,2
fld-1 (Col)	36,6 ± 6	117,2 ± 8,5
hos1-3 fld-1	16,8 ± 3,3	110,4 ± 4,9
siz1-2 (Col)	10,2 ± 1,1	16 ± 2,3
hos1-3 siz1-2	7,4 ± 0,6	13,7 ± 3,1
fha-1 (Ler)	12,5 ± 0,8	
hos1-2 fha-1	8,7 ± 0,8	
gi-3 (Ler)	25 ± 2	
hos1-2 gi-3	18,6 ± 1,2	
co-2 (Ler)	21,8 ± 5,9	23,4 ± 2,7
hos1-2 co-2	20,1 ± 1,3	14 ± 2,2
co-10 (Col)	38,6 ± 10,9	
hos1-3 co-10	26 ± 6,9	
cop1-4 (Col)	11,8 ± 0,9	12,8 ± 1,6
hos1-3 cop1-4	5 ± 0,6	5,1 ± 1
cop1-4 co-10	28,9 ± 4,2	
hos1-3 cop1-4 co-10	20,3 ± 3,2	
fkf1-1 (Col)	46,1 ± 6,1	
hos1-3 fkf1-1	17,5 ± 1,8	
Col [35S::CO]	4 ± 0	
hos1-3 [35S::CO]	4,1 ± 0,3	
ft-1 (Ler)	17,3 ± 1,9	39,2 ± 4,8
hos1-2 ft-1	16,7 ± 0,8	35,9 ± 2,9
soc1-1 (Ler)	14 ± 1,9	56,2 ± 5,3
hos1-2 soc1-1	10,2 ± 0,6	30,2 ± 5,4
ft-1 soc1-1	37,2 ± 3,3	
hos1-2 ft-1 soc1-1	32,6 ± 2,9	

Table 1. Total number of leaves at the time of flowering for the different wild-type ecotypes and single, double and triple mutants described in this work. Data were scored in approximately 30 plants under LD conditions and 15 plants under SD photoperiods and is represented as mean ± s.e.m.

SUPPLEMENTAL TABLES

Supplemental Table 1. Polymorphic molecular markers used for *esd6* mapping

Marker	Type	BAC clone	Primer 1	Primer 2
nga168	SSLP	T7F6	TCGTCTACTGCACTGCCG	GAGGACATGTATAGGAGCCTCG
T16B24	SSLP	T16B24	GCTATTGGTGATGAACGGAG	CATTTGACACTTTCGCGTAG
F12L6	SSLP	F12L6	CCCTGAACTTCACATCTGCTGCAAC	GGTTTCAGTAGTGGTTCTCGTTTAGG
C005	SSLP	T5I7	AATTATCGCACCTAGTTGAGG	TTGTATGAAGGATCATCTGCC
T5I7	SSLP	T5I7	GCGTCTGCACTATGAAATGTTTCG	CCGGAACTTGACCCATATCG
T28M21	SSLP	T28M21	CCGCCACCGAAGCTAAGAATCG	CGACACATCTAAGCAAACACATTCTTATC
T7D17	dCAP	T7D17	GCCATAAGGAACTTTTTGTC	GAGGACATCTTTATCAAACC
T3K9	SSNP	T3K9	GACGAACTTCCAATGGCGGAGGT	CGCTGCCGCCGGGCTTTTGGCTCG

Supplemental Table 2. Flowering time of *hos1* double mutants

	1 week 4ºC	4 weeks 4ºC
Ler	9,4 ± 0,9	10,2 ± 1
hos1-2	8,5 ± 1	9,6 ± 0,9
fca-1	23,4 ± 1,3	11,2 ± 0,8
hos1-2 fca-1	13 ± 1,3	10,4 ± 1,9
vrn1-2 fca-1	42,5 ± 6,2	31,2 ± 4,7
hos1-2 vrn1-2 fca-1	15,1 ± 2	14,7 ± 3,2
Col	12 ± 1	9,1 ± 0,9
hos1-3	8,1 ± 0,6	6,7 ± 0,5
Col FRI Sf-2	66,7 ± 11,6	18,6 ± 2,1
hos1-3 FRI Sf-2	31,6 ± 5,8	9 ± 1,2
vin3-4 FRI Sf-2	76,5 ± 11,4	80,1 ± 10,1
hos1-3 vin3-4 FRI Sf-2	39,8 ± 7,2	43,9 ± 8,8

Number of leaves was scored in approximately 12 plants under
LD conditions and is represented as mean ± s.e.m.

Supplemental Table 3. Flowering time of
transgenic plants bearing a *CO-LUC* construct

Col	13,2 ± 0,9
hos1-3	7,5 ± 0,6
35S::CO-LUC 6-2/Col	5,9 ± 0,3
35S::CO-LUC 6-2/hos1-3	4,6 ± 0,4

Number of leaves was scored in approximately 10 plants under
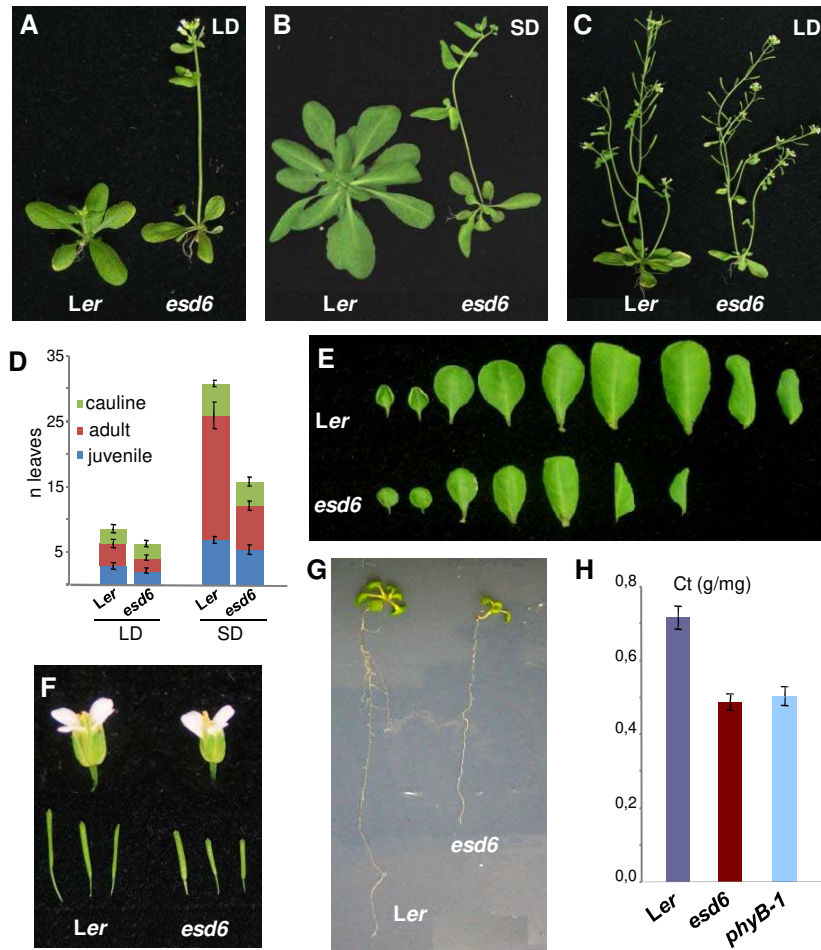LD conditions and is represented as mean ± s.e.m.

Figure 1. Phenotypic characterization of the *esd6* mutant.
(A,B) Flowering time phenotype of L*er* and *esd6* plants grown in LD conditions for 23 days (A) or in SD conditions for 54 days (B). (C) Phenotype of L*er* and *esd6* plants grown in LD conditions for 35 days (D) Histograms comparing the number of juvenile, adult and cauline leaves in L*er* and *esd6* plants grown under both LD and SD photoperiods. (E) Rosette and cauline leaves of L*er* and *esd6* plants grown in LDs. (F) Detached L*er* and *esd6* flowers and siliques from plants grown under LD conditions. (G) Root elongation in 11 day-old L*er* and *esd6* seedlings. (H) Total chlorophyll content (Ct) in L*er* and *esd6* and *phyB-1* mutant seedlings.

Figure 2. Identification of *ESD6*.
(A) Map-based cloning of *ESD6*. The genetic interval and the bacterial artificial chromosome (BAC) clones in the genomic region surrounding *ESD6* are shown. The number of recombinant events between molecular markers is given in parentheses. The position of *HOS1* ORF in T5I7 BAC clone is indicated. (B) Scheme of the *ESD6/HOS1* gene structure showing the polymorphisms associated to the different *hos1* mutant alleles isolated. Exons are represented by squared boxes, while introns are drawn by a line. (C) Pictures illustrating the flowering time of *hos1* mutants and their respective wild-type genotypes in LD and SD conditions. Plants were grown for 23 days under LD conditions (upper panel). SD pictures (lower panel) were taken after 64 days for C24 and *hos1-1*, 58 days for L*er* and *hos1-2* and 60 days for Col and *hos1-3*.
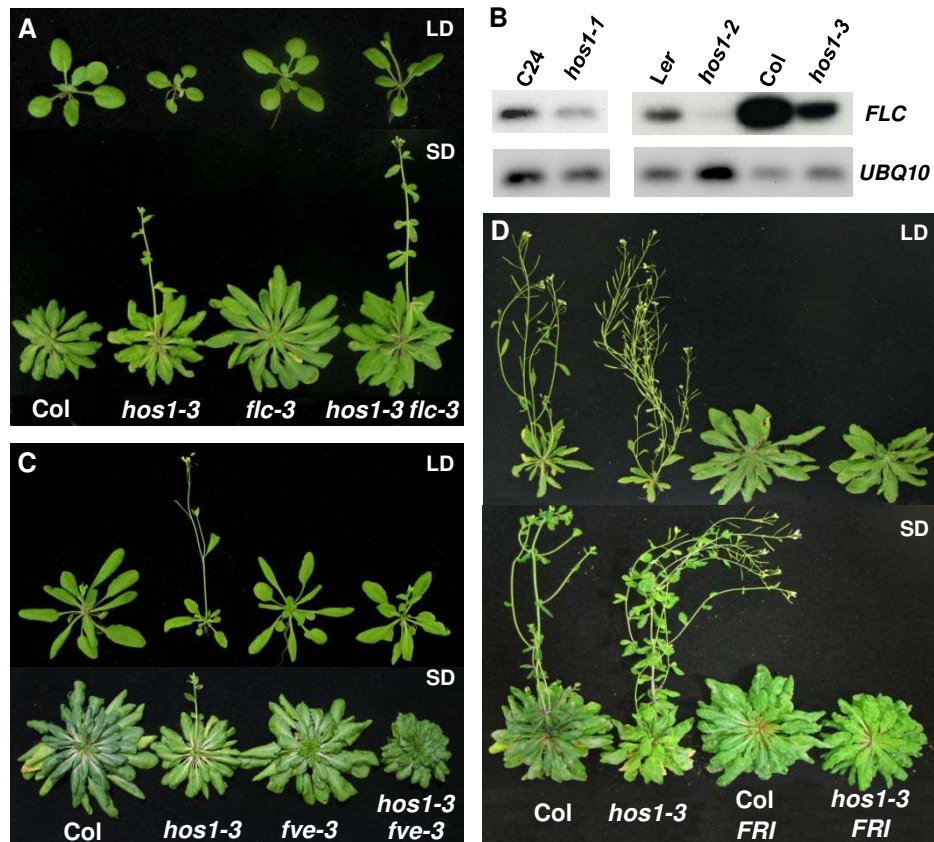
Figure 3. *hos1* mutations downregulate *FLC* expression and have an *FLC*-independent effect in the control of flowering time.

(A) Flowering time phenotype of *hos1-3 flc-3* double mutant in LD (upper panel) and SD (lower panel) conditions. (B) Analysis of the expression of *FLC* in 14 day-old *hos1* mutant seedlings and their corresponding wild-type genotypes. *FLC* expression was monitored by semiquantitative RT-PCR analysis over 22 cycles for C24 and *hos1-1* and over 28 cycles for L*er*, *hos1-2*, Col and *hos1-3*. For the *UBQ10* control 22 cycles were used. (C) Flowering time phenotype of *hos1-3 fve-3* double mutant plants grown in LD (upper panel) and SD (lower panel) conditions. (D) Flowering time phenotype of *hos1-3* plants bearing an active allele of *FRI* in LDs (upper panel) and SDs (lower panel).
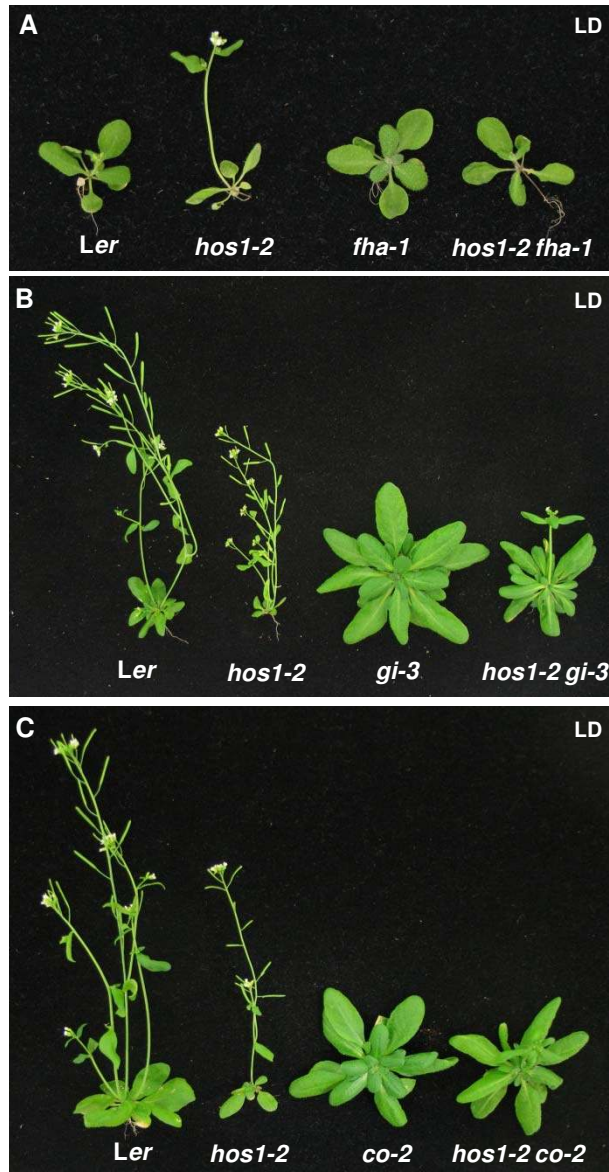
Figure 4. Genetic analyses between *hos1* and mutations in photoperiod pathway genes.
Flowering time phenotype of *hos1-2 fha-1* (A), *hos1-2 gi-3* (B) and *hos1-2 co-2* (C) double mutants grown in LD conditions.
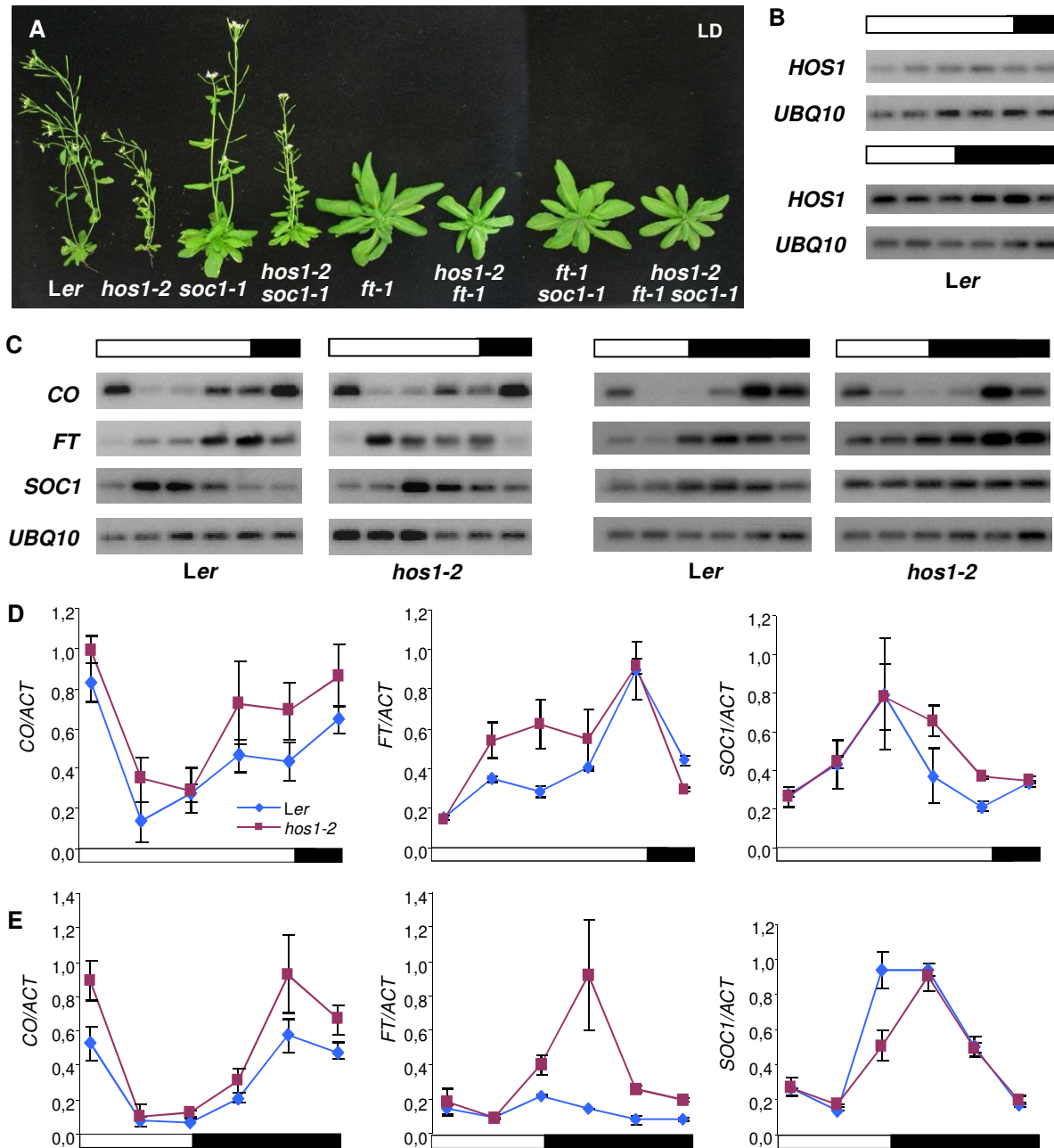
Figure 5. The early flowering phenotype of *hos1* depends on FT and SOC1 functional proteins and *hos1* mutation alters the pattern of expression of *FT*.
(A) Flowering time phenotype of *hos1-2 soc1-1*, *hos1-2 ft-1* and *hos1-2 ft-1 soc1-1* triple mutant plants grown in LD conditions. (B) *HOS1* expression pattern over a 24h time course in L*er* seedlings grown for 8 days in LDs and for 16 days in SDs. Samples were harvested every 4h after dawn. *HOS1* expression was monitored by semiquantitative RT-PCR analysis over 20 cycles. (C, D, E) Expression analysis of different flowering time genes over a 24h time course in L*er* and *hos1-2* seedlings grown for 8 days in LDs and 16 days in SDs. Samples were harvested every 4h after dawn (C) Semiquantitative RT-PCR analysis comparing *CO* (22 cycles), *FT* (28 cycles) and *SOC1* (24 cycles) expression (D) Quantitative real-time PCR (Q-PCR) analysis of *CO*, *FT* and *SOC1* expression in LD conditions (E) Same as (D) but L*er* and *hos1-2* seedlings grown in SD conditions. Relative expression levels were normalized to *β-ACTIN* expression.
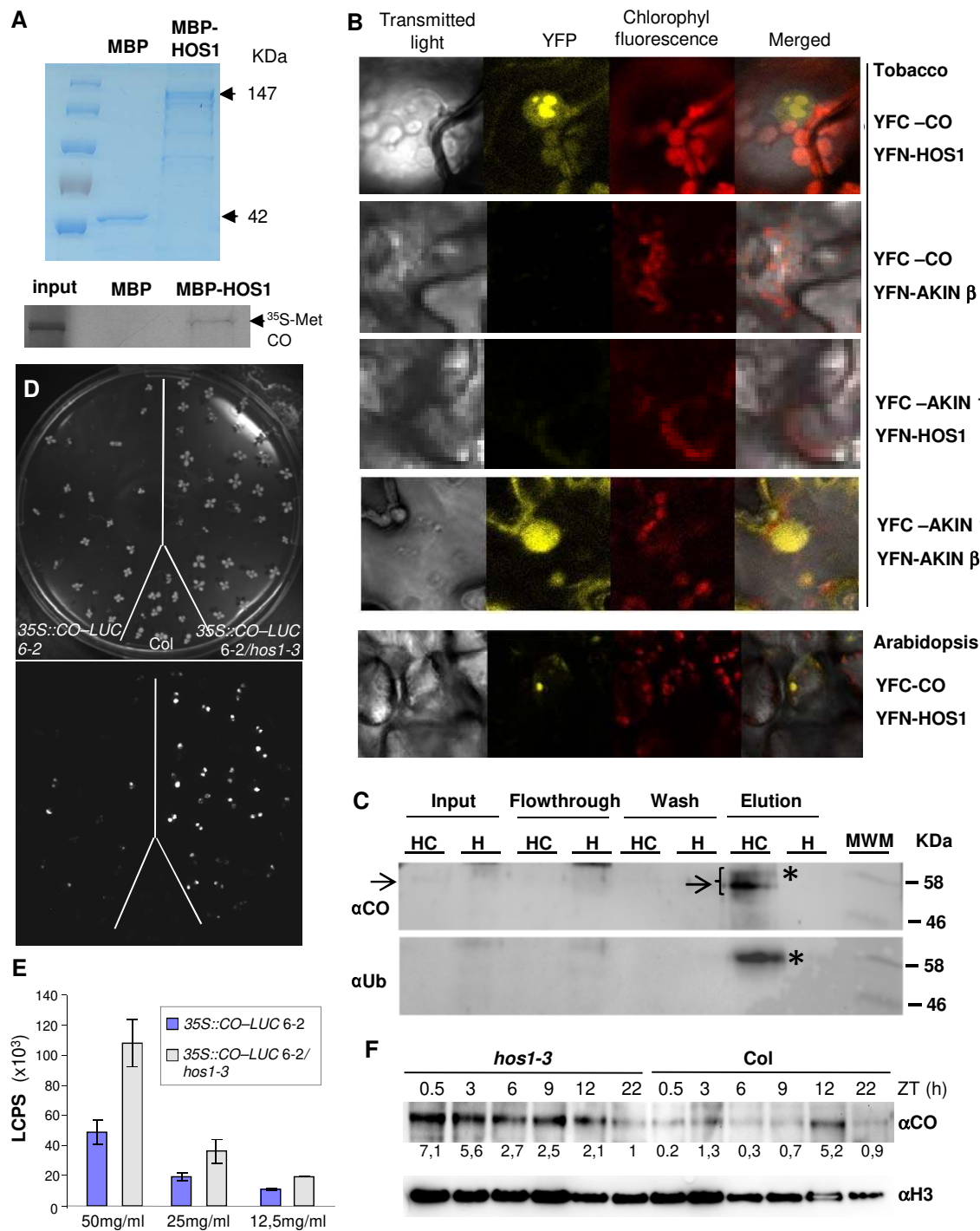
Figure 6. HOS1 interacts with CO and regulates its abundance.
(A) HOS1 and CO interact *in vitro*. A Coomassie stained SDS-PAGE showing MBP (42KDa) and MBP-HOS1 fusion protein (147KDa) expressed in *Escherichia coli BL21* Rosetta strain and purified on amylose resin is shown in the upper panel. The lower panel shows the result of a pull-down assay with MBP and MBP-HOS1 proteins incubated with ^{35}S-Met-labelled CO protein. Retained CO protein was visualized after autoradiography of the dried gel. (B) HOS1 interacts with CO *in planta*. BiFC assay co-expressing the C terminus of YFP fused to CO (CO-YFC) and the N terminus of YFP to HOS1 (YFN-HOS1) in tobacco and Arabidopsis leaves. Yellow fluorescence in the nucleus was indicative of interaction. Negative and positive controls were included in the assay. (C) *In vivo* coimmunoprecipitation between HOS1 and CO. GFP-HOS1 protein was immunoprecipitated from *35S::CO 35S::GFP-HOS1* (HC) and *35S::GFP-HOS1* (H) plants employing GFP antibody-agarose columns and detected with anti-CO antibodies (Elution HC, upper panel). The arrow marks both the co-immunoprecipitated CO protein and input. Antibodies against ubiquitin recognized, in the same blot, a higher molecular mass band (asterisk) corresponding to an ubiquitinated CO form (Elution HC, lower panel). Controls included input (1/50) from HC and H samples as well as column flowthrough and washes. Protein markers are shown on the right. (D) Non invasive *in vivo* luciferase imaging of *35S::CO–LUC* 6-2 and *35S::CO–LUC* 6-2/*hos1-3* seedlings. Pictures show 7 day-old seedlings grown in LDs 3 h after the lights are on. At this time, more CO-LUC protein accumulates in *hos1* mutant (below right) than in the wild-type (below left). (E) Quantification of the luciferase activity in *35S::CO–LUC* 6-2 (blue bars) and *35S::CO–LUC* 6-2/*hos1-3* (grey bars) seedlings expressed as luciferase counts per second (LCPS) in serial dilutions of fresh tissue in Steadylite Plus Reagent (mg/ml). (F) Immunoblot showing CO protein levels during a 24 h time course in nuclear extracts from Col and *hos1-3* plants grown under LDs. Numbers above each lane represent hours after dawn that the sample was harvested. Histone H3 was used as a loading control. Relative quantification of each band compared to the control is expressed below the upper panel (α-CO).
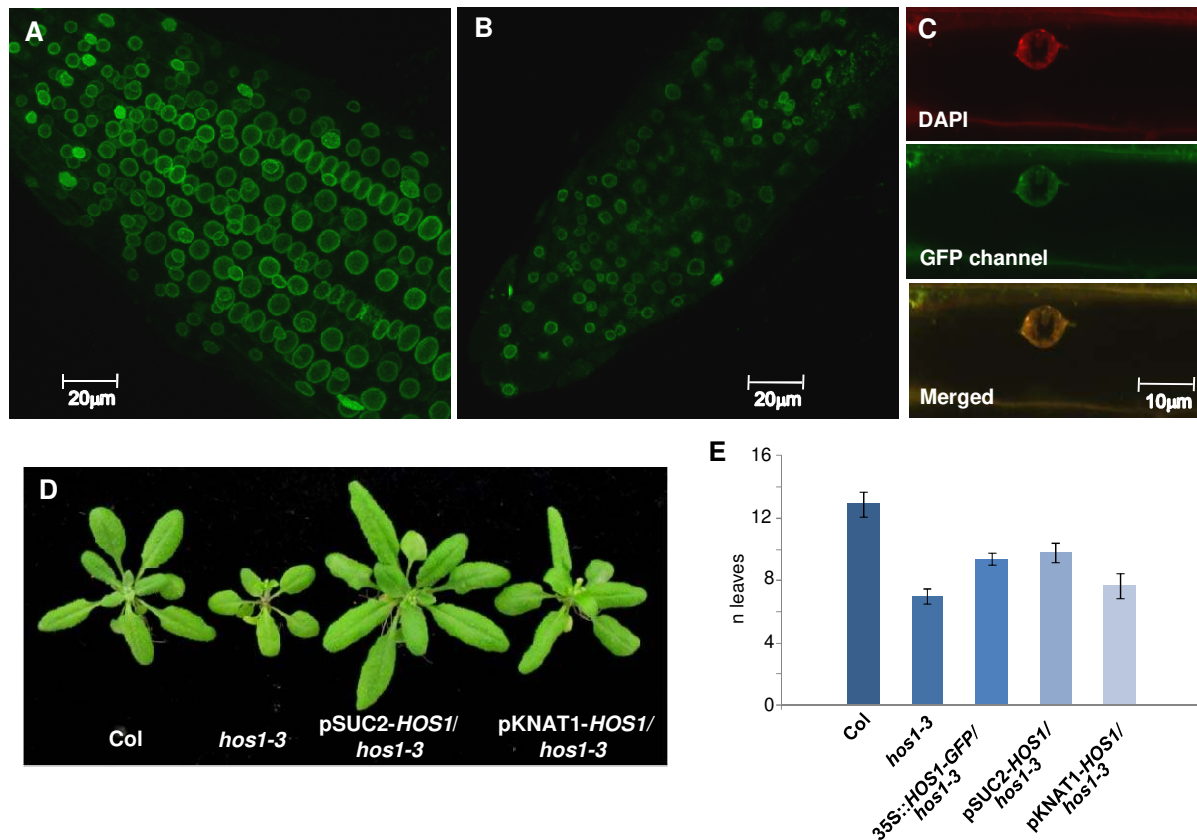
Figure 7. HOS1 is a nuclear-localized protein that exerts an effect in the phloem to regulate photoperiodic flowering
Localization of HOS1-GFP in the root cells of 10-day old *35S::HOS1-GFP/hos1-3* plants analysed under confocal microscopy. (A) Plants grown under continuous light. (B) Plants grown in darkness. (C) A representative nuclear image of a light-grown seedling showing DAPI staining (upper panel), GFP fluorescence (middle panel) and the merge of both images (lower panel). Tissue specific expression of *HOS1* in phloem companion cells and in the shoot apical meristem of *hos1* transgenic plants. (D) Flowering time phenotype of Col, *hos1-3, SUC2::HOS1/hos1-3 and KNAT1::HOS1/hos1-3* plants in LD. (E) Quantification of flowering time of Col, *hos1-3, 35S::HOS1-GFP/hos1-3*, *SUC2::HOS1/hos1-3 and KNAT1::HOS1/hos1-3* plants grown in LD conditions. Total number of leaves was scored in approximately 10 plants and is represented as mean ± s.e.m.
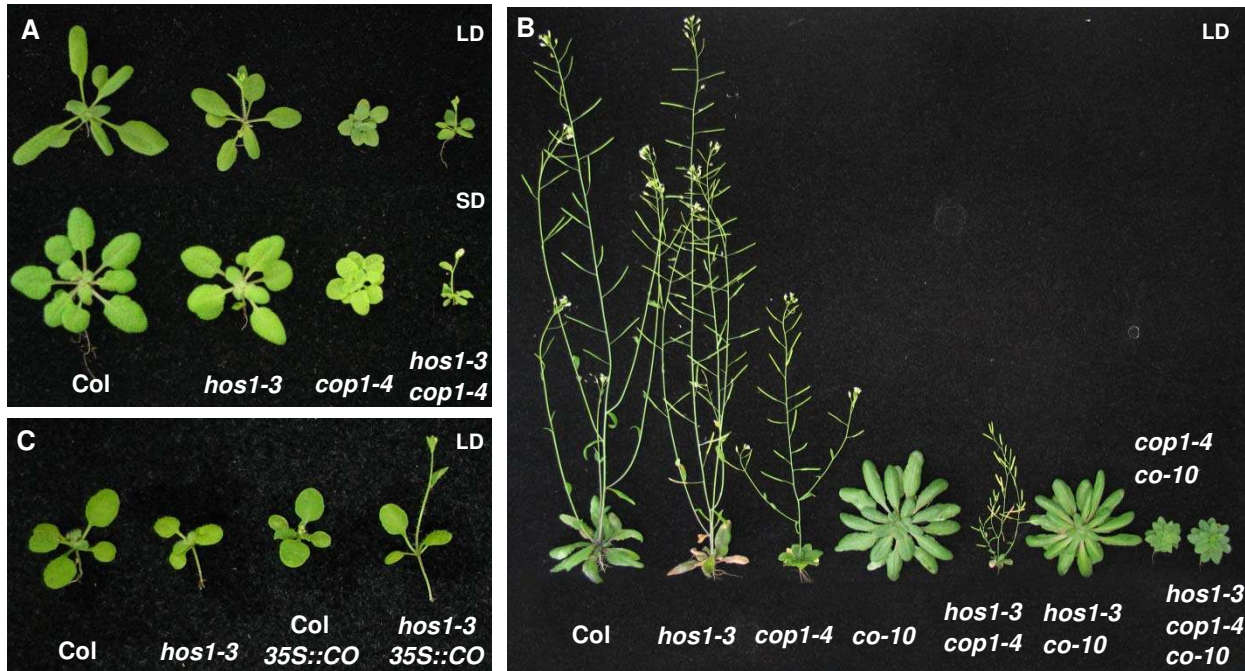
Figure 8. Genetic interaction between *HOS1* and *COP1* in the control of flowering time.
(A) Flowering time phenotype of *hos1-3 cop1-4* double mutant in LD (upper panel) and SD (lower panel) conditions. (B) Flowering time phenotype of double and triple mutant combinations between *hos1-3 co-10 cop1-4* mutants grown in LD conditions. (C) Comparison of flowering time phenotype between LD-grown Col and *hos1-3* plants bearing a *35S::CO* transgene.
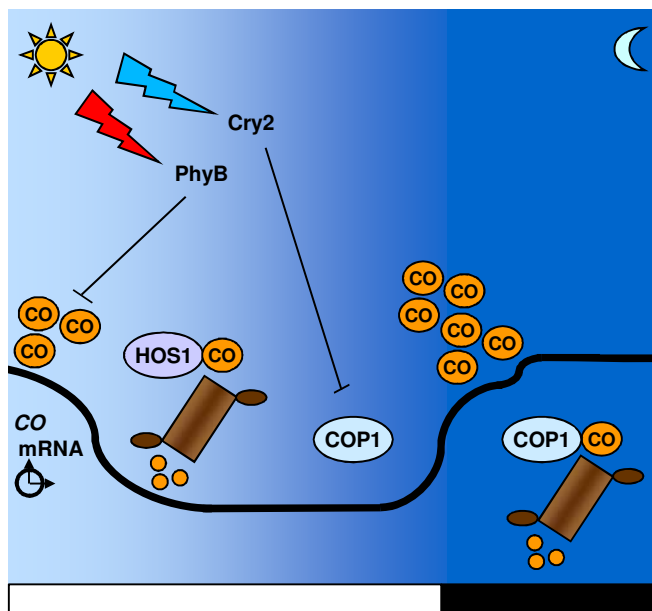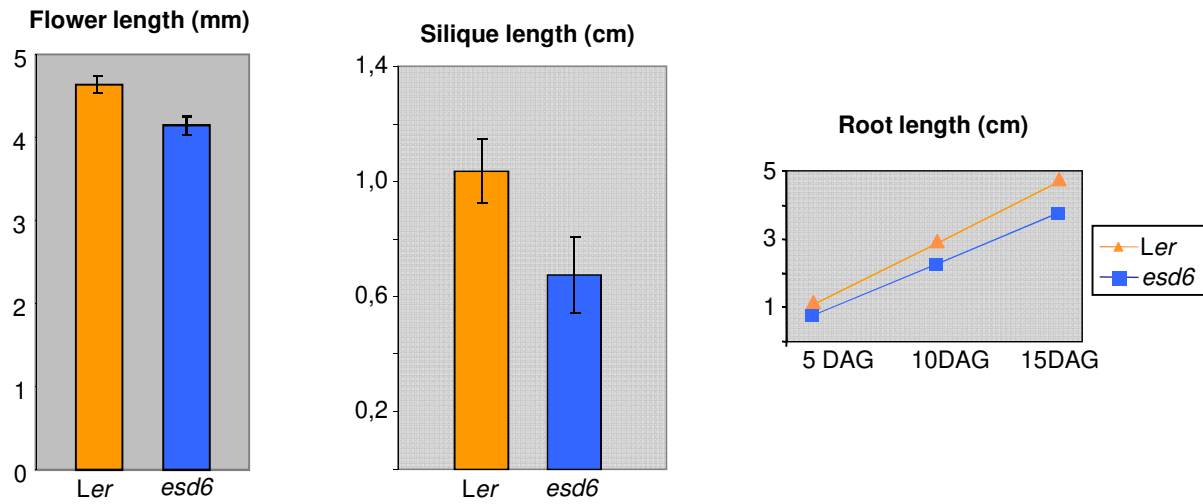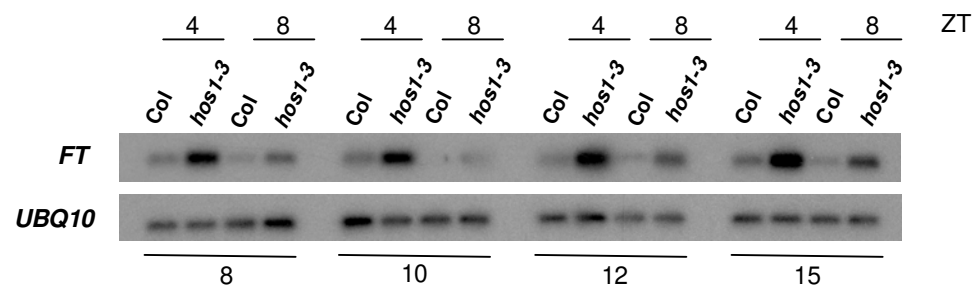
Figure 9. Model for HOS1 function in the photoperiodic control of flowering time.
The transcription of *CO* gene depends primarily on the circadian clock (thick black line). In the evening, the degradation of CDFs by the GI/FKF1 complex allows *CO* transcript levels to increase, and CO protein accumulates due to a photoreceptor-mediated repression of COP1. At this time CO can promote *FT* expression and induce flowering. During the night, COP1 activity causes rapid degradation of CO protein by the ubiquitination/26S proteasome system. In the daylight period HOS1 is required to degrade CO. Additional data will be necessary to establish the possible involvement of HOS1 in the mechanism of CO degradation mediated by PhyB that has been proposed to operate in the morning.

Flower length (mm)

Silique length (cm)

Root length (cm)

Supplemental Figure 1. Flower, silique and root length measurement in L*er* and *esd6*.
Data were scored on an average of 10 plants grown under LD conditions.

Supplemental Figure 2. Sequence comparison of Arabidopsis HOS1 (AtHOS1) with the HOS1 orthologues from *Ricinus communis* (RcHOS1), *Populus trichocarpa* (PtHOS1), *Citrus trifoliate* (CtHOS1), *Vitis vinifera* (VvHOS1), *Oryza sativa* (OsHOS1) and *Physcomytrella patents* (PpHOS1).
Amino acid residues in black are identical, and those in grey are functionally similar in the sequences. The conserved cysteine residues in the RING finger domain are indicated with black triangles. The putative nuclear localization signal present in the C terminal region of HOS1 is underlined. Genbank accession numbers are NP_181511 for AtHOS1, XP_002531460 for RcHOS1, XP_002304293 for PtHOS1, ACY92092 for CtHOS1, XP_002264751 for VvHOS1, AAR07079 for OsHOS1 and XP_001780235 for PpHOS1.

Supplemental Figure 3. *FT* expression analysis in LD grown Col and *hos1-3* seedlings harvested 4 and 8 h after dawn at 8, 10, 12 and 15 DAG.

Supplemental figure for reviewers letter
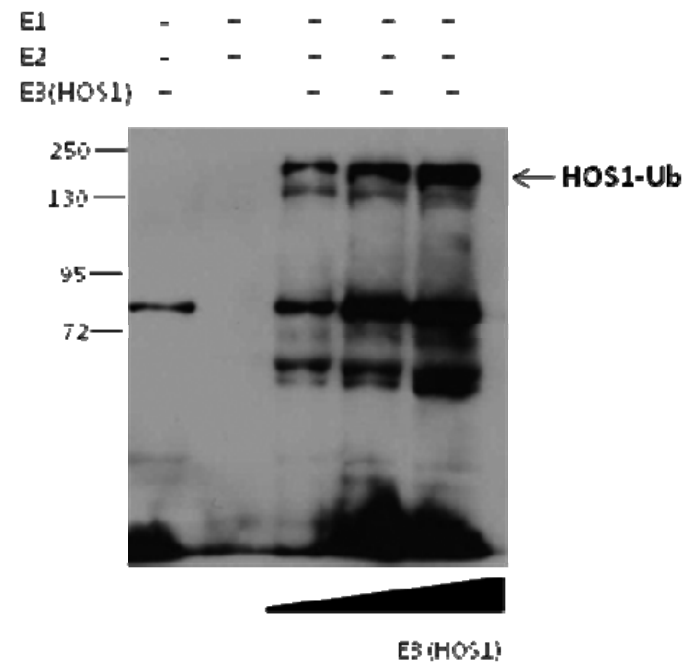
Membrane probed against an anti-ubiquitin antibody